Aspects of Hyperscaling Violating Geometries at Finite Radial Cutoff

Farzad Omidi

School of Physics, Institute for Research in Fundamental Sciences (IPM),Tehran,

School of Particles and Accelerators, IPM,
3 November 2021

References and Acknowledgment:

This talk is based on:
S. Khoeini-Moghaddam, F. Omidi, Chandrima Paul, "Aspects of Hyperscaling Violating Geometries at Finite Cutoff",
JHEP 02 (2021) 121, arXiv: 2011.00305 [hep-th].

References and Acknowledgment:

This talk is based on:
S. Khoeini-Moghaddam, F. Omidi, Chandrima Paul, "Aspects of Hyperscaling Violating Geometries at Finite Cutoff",
JHEP 02 (2021) 121, arXiv: 2011.00305 [hep-th].

I would like to thank M. Alishahiha for very useful discussions.

Outline:

- $T\overline{T}$ deformed CFTs and their holographic duals

Outline:

- $T\overline{T}$ deformed CFTs and their holographic duals
- Hyperscaling Violating (HV) geometries at finite radial cutoff and their dual QFTs

Outline:

- $T\overline{T}$ deformed CFTs and their holographic duals
- Hyperscaling Violating (HV) geometries at finite radial cutoff and their dual QFTs
- Some measures of quantum entanglement and the corresponding holographic prescription:
  1. Entanglement Entropy (EE),
  2. Mutual Information (MI),
  3. Entanglement Wedge Cross Section (EWCS)

Outline:

- $T\overline{T}$ deformed CFTs and their holographic duals
- Hyperscaling Violating (HV) geometries at finite radial cutoff and their dual QFTs
- Some measures of quantum entanglement and the corresponding holographic prescription:
  1. Entanglement Entropy (EE),
  2. Mutual Information (MI),
  3. Entanglement Wedge Cross Section (EWCS)

Outline:

- $T\overline{T}$ deformed CFTs and their holographic duals
- Hyperscaling Violating (HV) geometries at finite radial cutoff and their dual QFTs
- Some measures of quantum entanglement and the corresponding holographic prescription:
  1. Entanglement Entropy (EE),
  2. Mutual Information (MI),
  3. Entanglement Wedge Cross Section (EWCS)
- HV geometries at zero temperature and finite radial cutoff

Outline:

- $T\overline{T}$ deformed CFTs and their holographic duals
- Hyperscaling Violating (HV) geometries at finite radial cutoff and their dual QFTs
- Some measures of quantum entanglement and the corresponding holographic prescription:
  1. Entanglement Entropy (EE),
  2. Mutual Information (MI),
  3. Entanglement Wedge Cross Section (EWCS)
- HV geometries at zero temperature and finite radial cutoff
- Conclusions

$T\overline{T}$ deformation of a CFT_{d+1}:

$T\overline{T}$ deformation: is a very interesting kind of irrelevant deformations of a QFT [Zamolodchikov '04, Smirnov, Zamolodchikov '16, Cavaglià, Negro, Szécsényi, Tateo '16]

$$S_0 \to S(\lambda), \qquad \frac{\partial S(\lambda)}{\partial \lambda} = \int d^2x \sqrt{g}\; T\overline{T}(x),$$

$T\overline{T}$ deformation of a CFT_{d+1}:

$T\overline{T}$ deformation: is a very interesting kind of irrelevant deformations of a QFT [Zamolodchikov '04, Smirnov, Zamolodchikov '16, Cavaglià, Negro, Szécsényi, Tateo '16]

$$S_0 \to S(\lambda), \qquad \frac{\partial S(\lambda)}{\partial \lambda} = \int d^2x\sqrt{g}\; T\overline{T}(x),$$

in 2d, the deformation operator is of dimension four and can be written as follows

$$T\overline{T}(x) = \lim_{y\to x}\Big(T^{\alpha\beta}(x)\,T_{\alpha\beta}(y) - T^{\alpha}_{\alpha}(x)\,T^{\beta}_{\beta}(y)\Big) - \sum_i A_i(x-y)\nabla_y O_i(y).$$

$T\overline{T}$ deformation of a CFT_{d+1}:

$T\overline{T}$ deformation: is a very interesting kind of irrelevant deformations of a QFT [Zamolodchikov '04, Smirnov, Zamolodchikov '16, Cavaglià, Negro, Szécsényi, Tateo '16]

$$S_0 \to S(\lambda), \qquad \frac{\partial S(\lambda)}{\partial \lambda} = \int d^2x\sqrt{g}\; T\overline{T}(x),$$

in 2d, the deformation operator is of dimension four and can be written as follows

$$T\overline{T}(x) = \lim_{y\to x}\Big(T^{\alpha\beta}(x)\,T_{\alpha\beta}(y) - T^{\alpha}_{\alpha}(x)\,T^{\beta}_{\beta}(y)\Big) - \sum_i A_i(x-y)\nabla_y O_i(y).$$

Factorization property:

$$\langle T\overline{T}\rangle = \langle T^{ij}\rangle\langle T_{ij}\rangle - \langle T^{i}_{i}\rangle^2,$$

$T\overline{T}$ deformation of a CFT_{d+1}:

$T\overline{T}$ deformation: is a very interesting kind of irrelevant deformations of a QFT [Zamolodchikov '04, Smirnov, Zamolodchikov '16, Cavaglià, Negro, Szécsényi, Tateo '16]

$$S_0 \to S(\lambda), \qquad \frac{\partial S(\lambda)}{\partial \lambda} = \int d^2x\sqrt{g}\; T\overline{T}(x),$$

in 2d, the deformation operator is of dimension four and can be written as follows

$$T\overline{T}(x) = \lim_{y\to x}\Big(T^{\alpha\beta}(x)\,T_{\alpha\beta}(y) - T^{\alpha}_{\alpha}(x)\,T^{\beta}_{\beta}(y)\Big) - \sum_i A_i(x-y)\nabla_y O_i(y).$$

Factorization property:

$$\langle T\overline{T}\rangle = \langle T^{ij}\rangle\langle T_{ij}\rangle - \langle T^{i}_{i}\rangle^2,$$

The remarkable feature of these deformations is that they are solvable. Some quantities of the deformed CFT such as energy spectrum can be calculated exactly.

$T\overline{T}$ deformation of a CFT_{d+1}:

$T\overline{T}$ deformation: is a very interesting kind of irrelevant deformations of a QFT [Zamolodchikov '04, Smirnov, Zamolodchikov '16, Cavaglià, Negro, Szécsényi, Tateo '16]

$$S_0 \to S(\lambda), \qquad \frac{\partial S(\lambda)}{\partial \lambda} = \int d^2x\sqrt{g}\; T\overline{T}(x),$$

in 2d, the deformation operator is of dimension four and can be written as follows

$$T\overline{T}(x) = \lim_{y\to x}\Big(T^{\alpha\beta}(x)\,T_{\alpha\beta}(y) - T^{\alpha}_{\alpha}(x)\,T^{\beta}_{\beta}(y)\Big) - \sum_i A_i(x-y)\nabla_y O_i(y).$$

Factorization property:

$$\langle T\overline{T}\rangle = \langle T^{ij}\rangle\langle T_{ij}\rangle - \langle T^{i}_{i}\rangle^2,$$

The remarkable feature of these deformations is that they are solvable. Some quantities of the deformed CFT such as energy spectrum can be calculated exactly.

Recently, analogues of it have been studied in higher dimensions and in one dimension [Taylor '16, Cardy '18, Bonelli, Doroud, Zhu '18, Hartman, Kruthoff, Shaghoulian, Tajdini '18, Gross, Kruthoff, Rolph, Shaghoulian '19]

Gravity dual to a $T\overline{T}$-deformed CFT:

AdS/CFT correspondence: a strongly coupled CFT_{d+1} with a large central charge, is equivalent (dual) to a classical gravity on an asymptotically AdS_{d+2} spacetime.

Gravity dual to a $T\overline{T}$-deformed CFT:

AdS/CFT correspondence: a strongly coupled CFT_{d+1} with a large central charge, is equivalent (dual) to a classical gravity on an asymptotically AdS_{d+2} spacetime.

The CFT lives at $r = 0$, where r is the radial coordinate of the bulk spacetime.

Gravity dual to a $T\overline{T}$-deformed CFT:

AdS/CFT correspondence: a strongly coupled CFT_{d+1} with a large central charge, is equivalent (dual) to a classical gravity on an asymptotically AdS_{d+2} spacetime.
The CFT lives at $r = 0$, where r is the radial coordinate of the bulk spacetime.

A $T\overline{T}$-deformed CFT_{d+1} is dual to a gravity theory in an asymptotically AdS_{d+2} spacetime at finite radial cutoff r_c [McGough, Mezei, Verlinde '16, Kraus, Liu, Marolf '18, Hartman, Taylor '18, Kruthoff, Shaghoulian, Tajdini '18].

Gravity dual to a $T\overline{T}$-deformed CFT:

AdS/CFT correspondence: a strongly coupled CFT_{d+1} with a large central charge, is equivalent (dual) to a classical gravity on an asymptotically AdS_{d+2} spacetime.
The CFT lives at $r = 0$, where r is the radial coordinate of the bulk spacetime.

A $T\overline{T}$-deformed CFT_{d+1} is dual to a gravity theory in an asymptotically AdS_{d+2} spacetime at finite radial cutoff r_c [McGough, Mezei, Verlinde '16, Kraus, Liu, Marolf '18, Hartman, Taylor '18, Kruthoff, Shaghoulian, Tajdini '18].

By calculating the renormalized Brown-York stress tensor when there are no matter fields in the bulk and the boundary manifold is flat, the radial-radial component of Einstein's equations leads to the following constraint

$$T^i_i = -4\pi G_N r_c^{d+1} \left(T^{ij} T_{ij} - \frac{1}{d} \left(T^i_i \right)^2 \right).$$

Gravity dual to a $T\overline{T}$-deformed CFT:

AdS/CFT correspondence: a strongly coupled CFT_{d+1} with a large central charge, is equivalent (dual) to a classical gravity on an asymptotically AdS_{d+2} spacetime.

The CFT lives at $r = 0$, where r is the radial coordinate of the bulk spacetime.

A $T\overline{T}$-deformed CFT_{d+1} is dual to a gravity theory in an asymptotically AdS_{d+2} spacetime at finite radial cutoff r_c [McGough, Mezei, Verlinde '16, Kraus, Liu, Marolf '18, Hartman, Taylor '18, Kruthoff, Shaghoulian, Tajdini '18].

By calculating the renormalized Brown-York stress tensor when there are no matter fields in the bulk and the boundary manifold is flat, the radial-radial component of Einstein's equations leads to the following constraint

$$T^i_i = -4\pi G_N r_c^{d+1} \left(T^{ij} T_{ij} - \frac{1}{d} \left(T^i_i \right)^2 \right).$$

Trace flow equation

$$T^i_i = -(d+1)\lambda X,$$

Gravity dual to a $T\overline{T}$-deformed CFT:

AdS/CFT correspondence: a strongly coupled CFT_{d+1} with a large central charge, is equivalent (dual) to a classical gravity on an asymptotically AdS_{d+2} spacetime.
The CFT lives at $r = 0$, where r is the radial coordinate of the bulk spacetime.

A $T\overline{T}$-deformed CFT_{d+1} is dual to a gravity theory in an asymptotically AdS_{d+2} spacetime at finite radial cutoff r_c [McGough, Mezei, Verlinde '16, Kraus, Liu, Marolf '18, Hartman, Taylor '18, Kruthoff, Shaghoulian, Tajdini '18].

By calculating the renormalized Brown-York stress tensor when there are no matter fields in the bulk and the boundary manifold is flat, the radial-radial component of Einstein's equations leads to the following constraint

$$T^i_i = -4\pi G_N r_c^{d+1} \left(T^{ij} T_{ij} - \frac{1}{d} \left(T^i_i \right)^2 \right).$$

Trace flow equation

$$T^i_i = -(d+1)\lambda X,$$

which gives

$$X = T^{ij} T_{ij} - \frac{1}{d} \left(T^i_i \right)^2.$$

Gravity dual to a $T\overline{T}$-deformed CFT:

AdS/CFT correspondence: a strongly coupled CFT_{d+1} with a large central charge, is equivalent (dual) to a classical gravity on an asymptotically AdS_{d+2} spacetime.
The CFT lives at $r = 0$, where r is the radial coordinate of the bulk spacetime.

A $T\overline{T}$-deformed CFT_{d+1} is dual to a gravity theory in an asymptotically AdS_{d+2} spacetime at finite radial cutoff r_c [McGough, Mezei, Verlinde '16, Kraus, Liu, Marolf '18, Hartman, Taylor '18, Kruthoff, Shaghoulian, Tajdini '18].

By calculating the renormalized Brown-York stress tensor when there are no matter fields in the bulk and the boundary manifold is flat, the radial-radial component of Einstein's equations leads to the following constraint

$$T^i_i = -4\pi G_N r_c^{d+1} \left(T^{ij} T_{ij} - \frac{1}{d} \left(T^i_i \right)^2 \right).$$

Trace flow equation

$$T^i_i = -(d+1)\lambda X,$$

which gives

$$X = T^{ij} T_{ij} - \frac{1}{d} \left(T^i_i \right)^2.$$

$$\lambda = \frac{4\pi G_N}{(d+1)} r_c^{d+1},$$

Gravity dual to a $T\overline{T}$-deformed CFT:

AdS/CFT correspondence: a strongly coupled CFT_{d+1} with a large central charge, is equivalent (dual) to a classical gravity on an asymptotically AdS_{d+2} spacetime.
The CFT lives at $r = 0$, where r is the radial coordinate of the bulk spacetime.

A $T\overline{T}$-deformed CFT_{d+1} is dual to a gravity theory in an asymptotically AdS_{d+2} spacetime at finite radial cutoff r_c [McGough, Mezei, Verlinde '16, Kraus, Liu, Marolf '18, Hartman, Taylor '18, Kruthoff, Shaghoulian, Tajdini '18].

By calculating the renormalized Brown-York stress tensor when there are no matter fields in the bulk and the boundary manifold is flat, the radial-radial component of Einstein's equations leads to the following constraint

$$T^i_i = -4\pi G_N r_c^{d+1} \left(T^{ij} T_{ij} - \frac{1}{d} \left(T^i_i \right)^2 \right).$$

Trace flow equation

$$T^i_i = -(d+1)\lambda X,$$

which gives

$$X = T^{ij} T_{ij} - \frac{1}{d} \left(T^i_i \right)^2.$$

$$\lambda = \frac{4\pi G_N}{(d+1)} r_c^{d+1},$$

Zero-cutoff case: when $r_c = \epsilon \to 0$, and the dual CFT is undeformed.

Hyperscaling Violating (HV) Geometries at Finite Radial cutoff

A $d+2$ dimensional HV geometry at zero temperature

$$ds^2 = \frac{R^2}{r_F^{2\frac{\theta}{d}}} r^{2(\frac{\theta}{d}-1)} \left(-r^{-2(z-1)}\, dt^2 + dr^2 + \sum_{i=1}^{d} dx_i^2 \right),$$

Hyperscaling Violating (HV) Geometries at Finite Radial cutoff

A $d+2$ dimensional HV geometry at zero temperature

$$ds^2 = \frac{R^2}{r_F^{2\frac{\theta}{d}}} r^{2(\frac{\theta}{d}-1)} \left(-r^{-2(z-1)} dt^2 + dr^2 + \sum_{i=1}^{d} dx_i^2 \right),$$

There are two exponents z and θ. The Lorentz and scaling symmetries in the dual QFT, dubbed HV QFT are broken.

Hyperscaling Violating (HV) Geometries at Finite Radial cutoff

A $d+2$ dimensional HV geometry at zero temperature

$$ds^2 = \frac{R^2}{r_F^{2\frac{\theta}{d}}} r^{2(\frac{\theta}{d}-1)} \left(-r^{-2(z-1)} dt^2 + dr^2 + \sum_{i=1}^{d} dx_i^2 \right),$$

There are two exponents z and θ. The Lorentz and scaling symmetries in the dual QFT, dubbed HV QFT are broken.

Hyperscaling Violating (HV) Geometries at Finite Radial cutoff

A $d+2$ dimensional HV geometry at zero temperature

$$ds^2 = \frac{R^2}{r_F^{2\frac{\theta}{d}}} r^{2(\frac{\theta}{d}-1)} \left(-r^{-2(z-1)} dt^2 + dr^2 + \sum_{i=1}^{d} dx_i^2 \right),$$

There are two exponents z and θ. The Lorentz and scaling symmetries in the dual QFT, dubbed HV QFT are broken. For $z=1$ and $\theta=0$, it reduces to an AdS_{d+2} spacetime.

Hyperscaling Violating (HV) Geometries at Finite Radial cutoff

A $d+2$ dimensional HV geometry at zero temperature

$$ds^2 = \frac{R^2}{r_F^{2\frac{\theta}{d}}} r^{2(\frac{\theta}{d}-1)} \left(-r^{-2(z-1)}\, dt^2 + dr^2 + \sum_{i=1}^{d} dx_i^2 \right),$$

There are two exponents z and θ. The Lorentz and scaling symmetries in the dual QFT, dubbed HV QFT are broken. For $z=1$ and $\theta=0$, it reduces to an AdS_{d+2} spacetime.
However, there are enough symmetries to find [Alishahiha, Faraji Astaneh '19]

$$z T_t^t + \frac{d_e}{d} T_i^i = 0,$$

where $d_e = d - \theta$.

Hyperscaling Violating (HV) Geometries at Finite Radial cutoff

A $d+2$ dimensional HV geometry at zero temperature

$$ds^2 = \frac{R^2}{r_F^{2\frac{\theta}{d}}} r^{2(\frac{\theta}{d}-1)} \left(-r^{-2(z-1)}\, dt^2 + dr^2 + \sum_{i=1}^{d} dx_i^2 \right),$$

There are two exponents z and θ. The Lorentz and scaling symmetries in the dual QFT, dubbed HV QFT are broken. For $z=1$ and $\theta=0$, it reduces to an AdS_{d+2} spacetime.
However, there are enough symmetries to find [Alishahiha, Faraji Astaneh '19]

$$z T_t^t + \frac{d_e}{d}\, T_i^i = 0,$$

where $d_e = d - \theta$.
At finite radial cutoff, from the radial-radial component of Einstein's equation one obtains [Alishahiha, Faraji '19]

$$z T_i^i + \frac{d_e}{d}\, T_i^i = -\frac{8\pi\, d_e\, G_N}{z(2d_e + z - 1)}\, r_c^{d_e+z} \left[z \left(T_t^t\right)^2 + \frac{d_e}{d}\, T_j^i T_i^j - \frac{1}{d_e} \left(z T_t^t + \frac{d_e}{d}\, T_i^i \right)^2 \right],$$

Hyperscaling Violating (HV) Geometries at Finite Radial cutoff

A $d+2$ dimensional HV geometry at zero temperature

$$ds^2 = \frac{R^2}{r_F^{2\frac{\theta}{d}}} r^{2(\frac{\theta}{d}-1)} \left(-r^{-2(z-1)}\, dt^2 + dr^2 + \sum_{i=1}^{d} dx_i^2 \right),$$

There are two exponents z and θ. The Lorentz and scaling symmetries in the dual QFT, dubbed HV QFT are broken. For $z=1$ and $\theta=0$, it reduces to an AdS_{d+2} spacetime.
However, there are enough symmetries to find [Alishahiha, Faraji Astaneh '19]

$$z T_t^t + \frac{d_e}{d} T_i^i = 0,$$

where $d_e = d - \theta$.
At finite radial cutoff, from the radial-radial component of Einstein's equation one obtains [Alishahiha, Faraji '19]

$$z T_i^i + \frac{d_e}{d} T_i^i = -\frac{8\pi\, d_e\, G_N}{z(2d_e + z - 1)} r_c^{d_e+z} \left[z \left(T_t^t\right)^2 + \frac{d_e}{d} T_j^i T_i^j - \frac{1}{d_e} \left(z T_t^t + \frac{d_e}{d} T_i^i \right)^2 \right],$$

A $d+2$ dimensional HV geometry at finite radial cutoff might be dual to a HV QFT deformed by [Alishahiha, Faraji '19]

$$X = z \left(T_t^t\right)^2 + \frac{d_e}{d} T_j^i T_i^j - \frac{1}{d_e} \left(z T_t^t + \frac{d_e}{d} T_i^i \right)^2.$$

Hyperscaling Violating (HV) Geometries at Finite Radial cutoff

A $d+2$ dimensional HV geometry at zero temperature

$$ds^2 = \frac{R^2}{r_F^{2\frac{\theta}{d}}} r^{2(\frac{\theta}{d}-1)} \left(-r^{-2(z-1)}\, dt^2 + dr^2 + \sum_{i=1}^{d} dx_i^2 \right),$$

There are two exponents z and θ. The Lorentz and scaling symmetries in the dual QFT, dubbed HV QFT are broken. For $z=1$ and $\theta=0$, it reduces to an AdS_{d+2} spacetime.
However, there are enough symmetries to find [Alishahiha, Faraji Astaneh '19]

$$z T^t_t + \frac{d_e}{d}\, T^i_i = 0,$$

where $d_e = d-\theta$.
At finite radial cutoff, from the radial-radial component of Einstein's equation one obtains [Alishahiha, Faraji '19]

$$z T^i_i + \frac{d_e}{d}\, T^i_i = -\frac{8\pi\, d_e\, G_N}{z(2d_e+z-1)}\, r_c^{d_e+z} \left[z\left(T^t_t\right)^2 + \frac{d_e}{d}\, T^i_j T^j_i - \frac{1}{d_e}\left(z T^t_t + \frac{d_e}{d}\, T^i_i \right)^2 \right],$$

A $d+2$ dimensional HV geometry at finite radial cutoff might be dual to a HV QFT deformed by [Alishahiha, Faraji '19]

$$X = z\left(T^t_t\right)^2 + \frac{d_e}{d}\, T^i_j T^j_i - \frac{1}{d_e}\left(z T^t_t + \frac{d_e}{d}\, T^i_i \right)^2.$$

How measures of quantum entanglement are affected in this theory?

Entanglement Entropy (EE):

Quantum Entanglement: Bell pairs:

$$|\Psi\rangle = \frac{|00\rangle + |11\rangle}{\sqrt{2}}$$

By making a measurement on the first electron, one can find out in which state is the second electron.

Entanglement Entropy (EE):

Quantum Entanglement: Bell pairs:

$$|\Psi\rangle = \frac{|00\rangle + |11\rangle}{\sqrt{2}}$$

By making a measurement on the first electron, one can find out in which state is the second electron.

How to verify quantitatively the state is entangled or untangled?

Entanglement Entropy (EE):

Quantum Entanglement: Bell pairs:

$$|\Psi\rangle = \frac{|00\rangle + |11\rangle}{\sqrt{2}}$$

By making a measurement on the first electron, one can find out in which state is the second electron.

How to verify quantitatively the state is entangled or untangled? Consider a quantum system (QM or QFT) whose Hilbert space is $\mathcal{H}$, and is described by a density matrix ρ_{total}.

Entanglement Entropy (EE):

Quantum Entanglement: Bell pairs:

$$|\Psi\rangle = \frac{|00\rangle + |11\rangle}{\sqrt{2}}$$

By making a measurement on the first electron, one can find out in which state is the second electron.

How to verify quantitatively the state is entangled or untangled? Consider a quantum system (QM or QFT) whose Hilbert space is $\mathcal{H}$, and is described by a density matrix ρ_{total}.

Decompose the system into two subsystems A and its compliment B.

$$\mathcal{H} = \mathcal{H}_A \otimes \mathcal{H}_B$$

Entanglement Entropy (EE):

Quantum Entanglement: Bell pairs:

$$|\Psi\rangle = \frac{|00\rangle + |11\rangle}{\sqrt{2}}$$

By making a measurement on the first electron, one can find out in which state is the second electron.

How to verify quantitatively the state is entangled or untangled? Consider a quantum system (QM or QFT) whose Hilbert space is $\mathcal{H}$, and is described by a density matrix ρ_{total}.

Decompose the system into two subsystems A and its compliment B.

$$\mathcal{H} = \mathcal{H}_A \otimes \mathcal{H}_B$$

Then one can define a reduced density matrix ρ_A for the subsystem A, by tracing out the states of the subsystem B.

$$\rho_A = Tr_B\left(\rho_{total}\right) = \sum_{i \in \mathcal{H}_B} \langle i|\rho_{total}|i\rangle$$

Entanglement Entropy (EE):

Quantum Entanglement: Bell pairs:

$$|\Psi\rangle = \frac{|00\rangle + |11\rangle}{\sqrt{2}}$$

By making a measurement on the first electron, one can find out in which state is the second electron.

How to verify quantitatively the state is entangled or untangled? Consider a quantum system (QM or QFT) whose Hilbert space is $\mathcal{H}$, and is described by a density matrix ρ_{total}.

Decompose the system into two subsystems A and its compliment B.

$$\mathcal{H} = \mathcal{H}_A \otimes \mathcal{H}_B$$

Then one can define a reduced density matrix ρ_A for the subsystem A, by tracing out the states of the subsystem B.

$$\rho_A = Tr_B\left(\rho_{total}\right) = \sum_{i \in \mathcal{H}_B} \langle i|\rho_{total}|i\rangle$$

Entanglement Entropy of A is defined as the Von-Neumann entropy for ρ_A

$$S_A^{(EE)} = -Tr\left(\rho_A \log \rho_A\right)$$

If $S_A^{(EE)} = 0$, there is no quantum entanglement between the degrees of freedom inside A and B. Otherwise, they are entangled together.

Ryu-Takayanagi Formula

Computation of EE in strongly coupled Quantum Field Theories is a very difficult task!

Ryu-Takayanagi Formula

Computation of EE in strongly coupled Quantum Field Theories is a very difficult task!
There is a spacelike, codimension two, minimal surface in the bulk whose area gives the EE [Ryu , Takayanagi '06 - Maldacena , Lewkowycz '13]

$$S_A^{(EE)} = \frac{Area(\Gamma_A)}{4G_N^{d+1}}$$

There is a quantum correction to it, which we omit here.

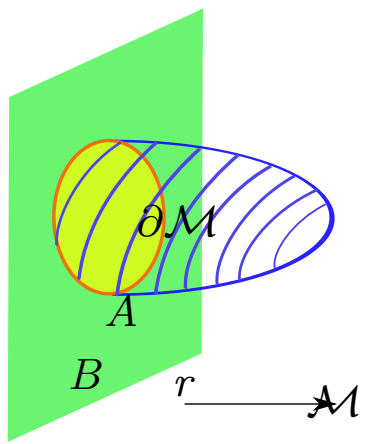

Mutual Information (MI)

EE depends on the UV cutoff of the QFT. Mutual Information is a measure of both classical and quantum correlations in a bipartite system $A \cup B$ and is defined by

$$I(A, B) = S_A + S_B - S_{A \cup B},$$

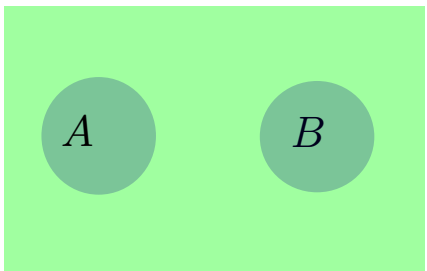

Mutual Information (MI)

EE depends on the UV cutoff of the QFT. Mutual Information is a measure of both classical and quantum correlations in a bipartite system $A \cup B$ and is defined by

$$I(A, B) = S_A + S_B - S_{A \cup B},$$

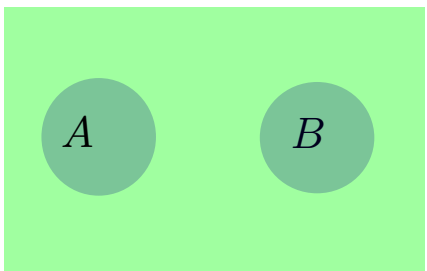

It has several interesting properties:

1. It is always non-negative as a result of subadditivity.

Mutual Information (MI)

EE depends on the UV cutoff of the QFT. Mutual Information is a measure of both classical and quantum correlations in a bipartite system $A \cup B$ and is defined by

$$I(A, B) = S_A + S_B - S_{A \cup B},$$

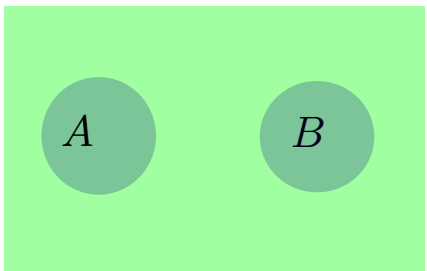

It has several interesting properties:

1. It is always non-negative as a result of subadditivity.
2. It is usually finite and independent of the UV cutoff.

Mutual Information (MI)

EE depends on the UV cutoff of the QFT. Mutual Information is a measure of both classical and quantum correlations in a bipartite system $A \cup B$ and is defined by

$$I(A, B) = S_A + S_B - S_{A \cup B},$$

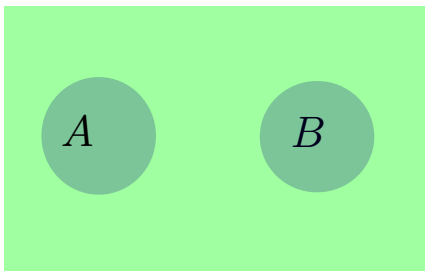

It has several interesting properties:

1. It is always non-negative as a result of subadditivity.
2. It is usually finite and independent of the UV cutoff.
3. It shows a first-order phase transition when the two subsystems becomes far enough from each other.

Mutual Information (MI)

EE depends on the UV cutoff of the QFT. Mutual Information is a measure of both classical and quantum correlations in a bipartite system $A \cup B$ and is defined by

$$I(A, B) = S_A + S_B - S_{A \cup B},$$

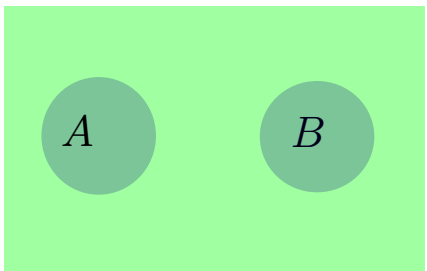

It has several interesting properties:

1. It is always non-negative as a result of subadditivity.
2. It is usually finite and independent of the UV cutoff.
3. It shows a first-order phase transition when the two subsystems becomes far enough from each other.
4. When the distance between the entangling regions goes to zero, it diverges.

Holographic Mutual Information (HMI):

To compute MI, one can apply holography

- S_A and S_B are simply given by:

$$S_{A,B} = \frac{Area(\Gamma_{A,B})}{4G_N}$$

Holographic Mutual Information (HMI):

To compute MI, one can apply holography

- S_A and S_B are simply given by:

$$S_{A,B} = \frac{Area(\Gamma_{A,B})}{4G_N}$$

- To calculate $S_{A\cup B}$, there are always two different configurations for the RT surfaces. They are called Connected and disconnected [Headrick '10].

$$S_{AB} = \text{Min}\left(S_{\text{con.}}, S_{\text{dis.}}\right),$$

Holographic Mutual Information (HMI):

To compute MI, one can apply holography

- S_A and S_B are simply given by:

$$S_{A,B} = \frac{Area(\Gamma_{A,B})}{4G_N}$$

- To calculate $S_{A\cup B}$, there are always two different configurations for the RT surfaces. They are called Connected and disconnected [Headrick '10].

$$S_{AB} = \text{Min}\left(S_{\text{con.}}, S_{\text{dis.}}\right),$$

The minimum depends on the size of A, B as well as the distance between them.

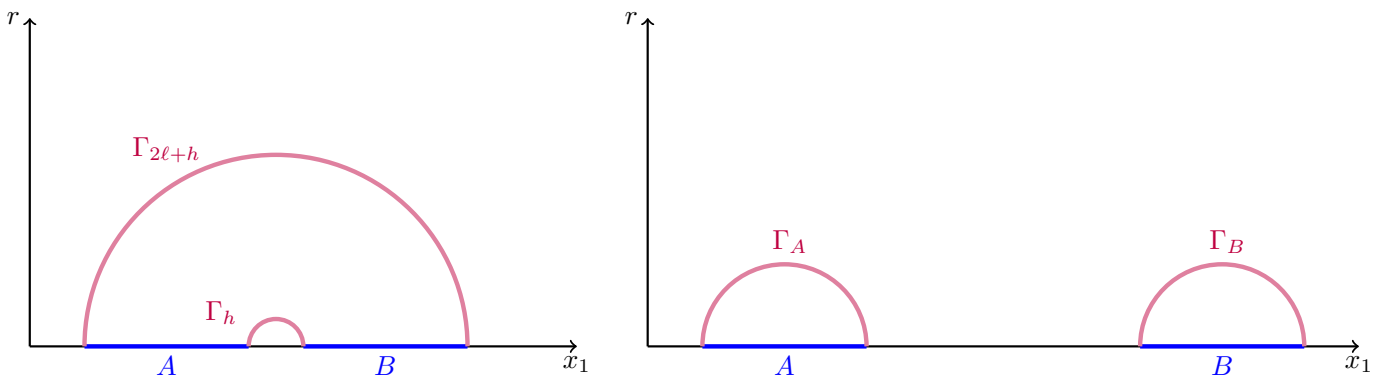

Holographic Mutual Information (HMI):

To compute MI, one can apply holography

- S_A and S_B are simply given by:

$$S_{A,B} = \frac{Area(\Gamma_{A,B})}{4G_N}$$

- To calculate $S_{A\cup B}$, there are always two different configurations for the RT surfaces. They are called Connected and disconnected [Headrick '10].

$$S_{AB} = \text{Min}\left(S_{\text{con.}}, S_{\text{dis.}}\right),$$

The minimum depends on the size of A, B as well as the distance between them.

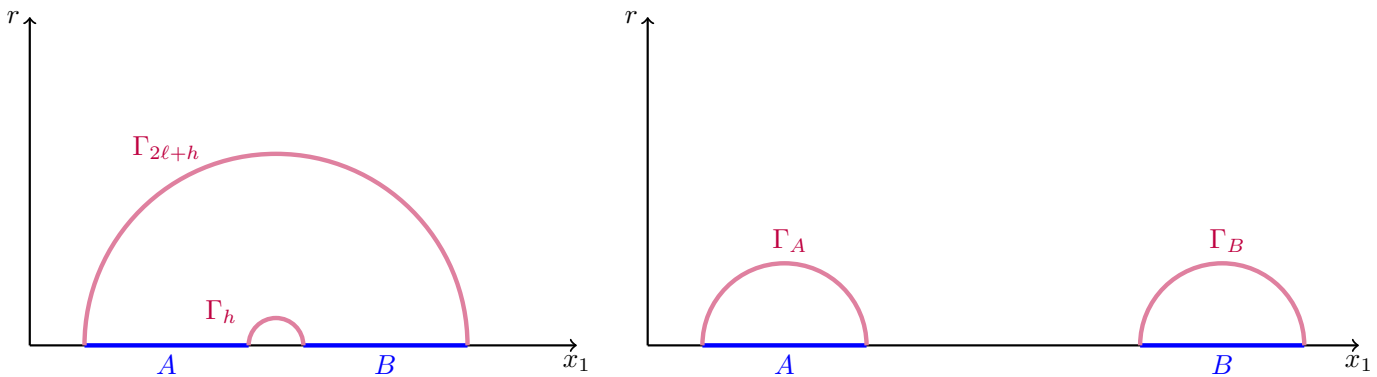

Therefore

$$I(A,B) = \begin{cases} 0 & \ell \ll h \\ 2S(\ell) - S(h) - S(2\ell+h) & \ell \gg h \end{cases}$$

Entanglement Wedge Cross Section (EWCS):

Entanglement wedge: is a region enclosed by null rays shoot from the RT surfaces toward the boundary of the bulk spacetime. Here we consider a constant time slice of the region.

Entanglement Wedge Cross Section (EWCS):

Entanglement wedge: is a region enclosed by null rays shoot from the RT surfaces toward the boundary of the bulk spacetime. Here we consider a constant time slice of the region.

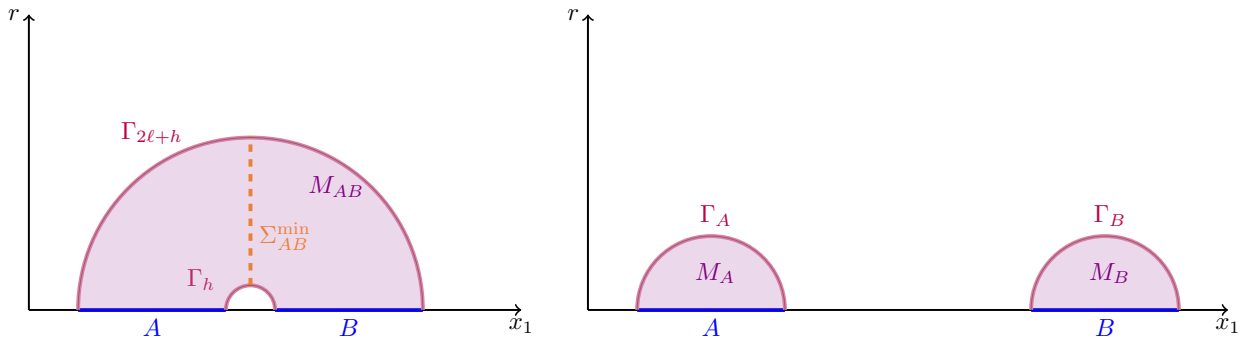

Entanglement Wedge Cross Section (EWCS):

Entanglement wedge: is a region enclosed by null rays shoot from the RT surfaces toward the boundary of the bulk spacetime. Here we consider a constant time slice of the region.

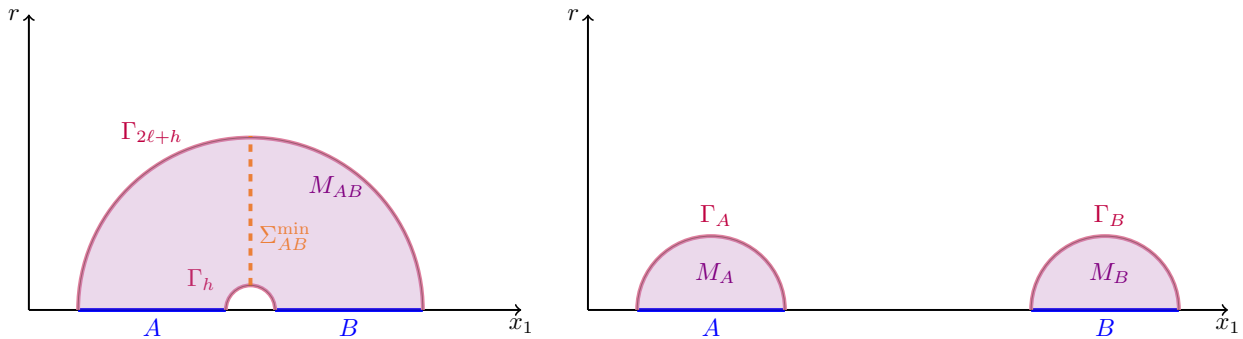

Entanglement wedge cross section (EWCS) is defined by [Takayanagi, Umemoto '17 - Nguyen, Devakul, Halbasch, Zaletel, Swingle '17]

$$E_W = \frac{Area(\Sigma_{AB}^{\min})}{4G_N},$$

$\Sigma_{AB}^{\min}$ is a minimal, codimension two, spacelike surface anchored on the connected RT surface $\Gamma_{2l+h} \cup \Gamma_l$.

Entanglement Wedge Cross Section (EWCS):

Entanglement wedge: is a region enclosed by null rays shoot from the RT surfaces toward the boundary of the bulk spacetime. Here we consider a constant time slice of the region.

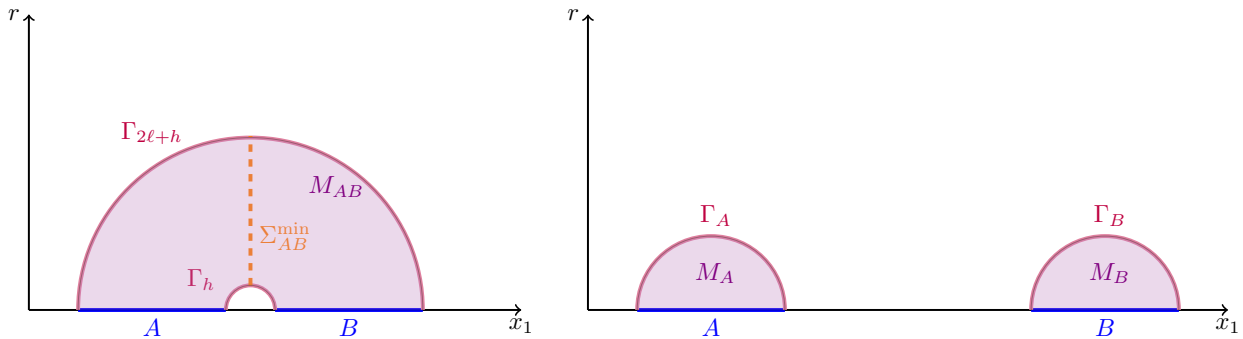

Entanglement wedge cross section (EWCS) is defined by [Takayanagi, Umemoto '17 - Nguyen, Devakul, Halbasch, Zaletel, Swingle '17]

$$E_W = \frac{Area(\Sigma_{AB}^{\min})}{4G_N},$$

$\Sigma_{AB}^{\min}$ is a minimal, codimension two, spacelike surface anchored on the connected RT surface $\Gamma_{2l+h} \cup \Gamma_l$.
EWCS has a variety of interesting properties including: It is

- non-negative and finite.

Entanglement Wedge Cross Section (EWCS):

Entanglement wedge: is a region enclosed by null rays shoot from the RT surfaces toward the boundary of the bulk spacetime. Here we consider a constant time slice of the region.

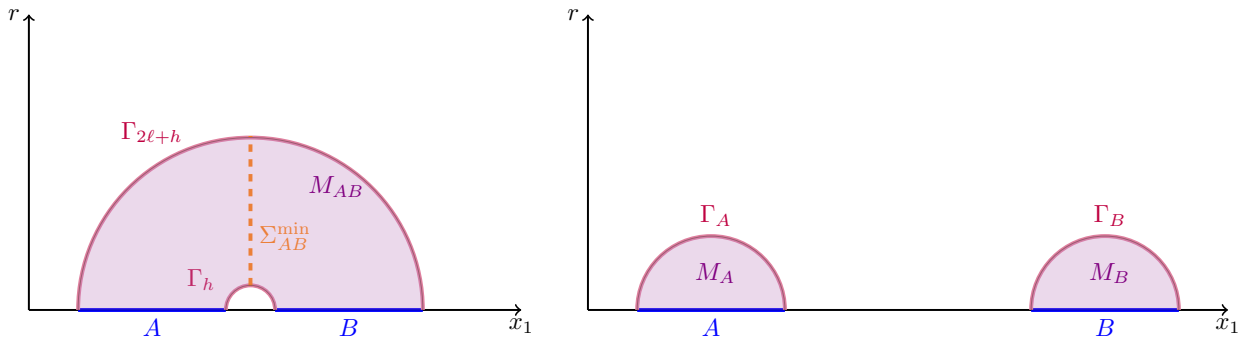

Entanglement wedge cross section (EWCS) is defined by [Takayanagi, Umemoto '17 - Nguyen, Devakul, Halbasch, Zaletel, Swingle '17]

$$E_W = \frac{Area(\Sigma_{AB}^{\min})}{4G_N},$$

$\Sigma_{AB}^{\min}$ is a minimal, codimension two, spacelike surface anchored on the connected RT surface $\Gamma_{2l+h} \cup \Gamma_l$.
EWCS has a variety of interesting properties including: It is

- non-negative and finite.
- independent of the UV cutoff.

Entanglement Wedge Cross Section (EWCS):

Entanglement wedge: is a region enclosed by null rays shoot from the RT surfaces toward the boundary of the bulk spacetime. Here we consider a constant time slice of the region.

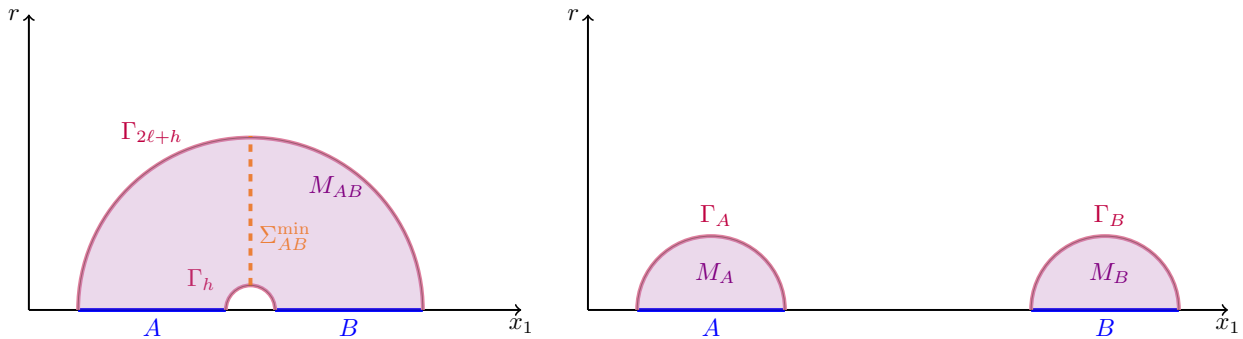

Entanglement wedge cross section (EWCS) is defined by [Takayanagi, Umemoto '17 - Nguyen, Devakul, Halbasch, Zaletel, Swingle '17]

$$E_W = \frac{Area(\Sigma_{AB}^{\min})}{4G_N},$$

$\Sigma_{AB}^{\min}$ is a minimal, codimension two, spacelike surface anchored on the connected RT surface $\Gamma_{2l+h} \cup \Gamma_l$.
EWCS has a variety of interesting properties including: It is

- non-negative and finite.
- independent of the UV cutoff.
- undergoes a discontinuous phase transition when the HMI shows a first-order phase transition.

- When ρ_{AB} is pure, one has $E_W = S_A = S_B$.
- it satisfies a variety of inequalities such as

$$E_W(\rho_{AB}) \geq \frac{I(A,B)}{2},$$

where the inequality is saturated, whenever ρ_{AB} is pure.

- When ρ_{AB} is pure, one has $E_W = S_A = S_B$.
- it satisfies a variety of inequalities such as

$$E_W(\rho_{AB}) \geq \frac{I(A,B)}{2},$$

where the inequality is saturated, whenever ρ_{AB} is pure.

What is the meaning of the EWCS on the CFT side?

- When ρ_{AB} is pure, one has $E_W = S_A = S_B$.
- it satisfies a variety of inequalities such as

$$E_W(\rho_{AB}) \geq \frac{I(A,B)}{2},$$

where the inequality is saturated, whenever ρ_{AB} is pure.

What is the meaning of the EWCS on the CFT side?
It may give Entanglement of Purification (EoP) for the two subsystems A and B [Takayanagi, Umemoto '17 - Nguyen, Devakul, Halbasch, Zaletel, Swingle '17]

$$E_P(\rho_{AB}) = E_W(\rho_{AB}).$$

- When ρ_{AB} is pure, one has $E_W = S_A = S_B$.
- it satisfies a variety of inequalities such as

$$E_W(\rho_{AB}) \geq \frac{I(A,B)}{2},$$

where the inequality is saturated, whenever ρ_{AB} is pure.

What is the meaning of the EWCS on the CFT side?
It may give Entanglement of Purification (EoP) for the two subsystems A and B [Takayanagi, Umemoto '17 - Nguyen, Devakul, Halbasch, Zaletel, Swingle '17]

$$E_P(\rho_{AB}) = E_W(\rho_{AB}).$$

EoP is a good measure of entanglement when the state is mixed and measures both classical and quantum correlations.

- When ρ_{AB} is pure, one has $E_W = S_A = S_B$.
- it satisfies a variety of inequalities such as

$$E_W(\rho_{AB}) \geq \frac{I(A,B)}{2},$$

where the inequality is saturated, whenever ρ_{AB} is pure.

What is the meaning of the EWCS on the CFT side?
It may give Entanglement of Purification (EoP) for the two subsystems A and B [Takayanagi, Umemoto '17 - Nguyen, Devakul, Halbasch, Zaletel, Swingle '17]

$$E_P(\rho_{AB}) = E_W(\rho_{AB}).$$

EoP is a good measure of entanglement when the state is mixed and measures both classical and quantum correlations.
Suppose that the density matrix ρ_{AB} of two subsystems A and B is mixed. By enlarging the Hilbert space to $\mathcal{H}_{AA'} \otimes \mathcal{H}_{BB'}$ in which A' and B' are two arbitrary subsystems, one can find a pure state $|\psi\rangle \in \mathcal{H}_{AA'} \otimes \mathcal{H}_{BB'}$, such that

$$\rho_{AB} = \mathrm{Tr}_{A'B'} |\psi\rangle\langle\psi|$$

$|\psi\rangle$ is called a purification of ρ_{AB}. EoP is defined by [Terhal, Horodecki, Leung, DiVincenzo '02]

$$E_P(\rho_{AB}) = \min_{\rho_{AB} = \mathrm{Tr}_{A'B'} |\psi\rangle\langle\psi|} S(\rho_{AA'}),$$

where $\rho_{AA'} = \mathrm{Tr}_{BB'} |\psi\rangle\langle\psi|$ and the minimization is done over all possible purifications of ρ_{AB}.

HEE for HV Geometry at Zero Temperature and Finite Radial Cutoff

We consider entangling regions in the shape of strips

$$-l/2 \leq x_1 \leq l/2, \qquad 0 \leq x_{2,3,\cdots,d} \leq L, \qquad t = const.$$

We consider entangling regions in the shape of strips

$$-l/2 \leq x_1 \leq l/2, \qquad 0 \leq x_{2,3,\cdots,d} \leq L, \qquad t = const.$$

the area functional is as follows

$$Area(\Gamma_A) = 2R^d L^{d-1} \int_{r_c}^{r_t} r^{-d_e} \sqrt{1 + x_1'(r)^2}\, dr,$$

We consider entangling regions in the shape of strips

$$-l/2 \leq x_1 \leq l/2, \qquad 0 \leq x_{2,3,\cdots,d} \leq L, \qquad t = const.$$

the area functional is as follows

$$Area(\Gamma_A) = 2R^d L^{d-1} \int_{r_c}^{r_t} r^{-d_e} \sqrt{1 + x_1'(r)^2}\, dr,$$

Minimizing the above functional gives a relation between r_t and ℓ as follows

$$\frac{\ell}{2} = \int_{r_c}^{r_t} \frac{dr\, r^{d_e}}{\sqrt{r_t^{2d_e} - r^{2d_e}}}$$

HEE for HV Geometry at Zero Temperature and Finite Radial Cutoff

We consider entangling regions in the shape of strips

$$-l/2 \leq x_1 \leq l/2, \qquad 0 \leq x_{2,3,\cdots,d} \leq L, \qquad t = const.$$

the area functional is as follows

$$Area(\Gamma_A) = 2R^d L^{d-1} \int_{r_c}^{r_t} r^{-d_e} \sqrt{1 + x_1'(r)^2}\, dr,$$

Minimizing the above functional gives a relation between r_t and ℓ as follows

$$\frac{\ell}{2} = \int_{r_c}^{r_t} \frac{dr\, r^{d_e}}{\sqrt{r_t^{2d_e} - r^{2d_e}}}$$

The HEE is given by

$$S = \frac{R^d L^{d-1}}{2G_N} \int_{r_c}^{r_t} \frac{dr}{r^{d_e}\sqrt{1 - \left(\frac{r}{r_t}\right)^{2d_e}}}.$$

We consider the two cases $d_e = 1$ and $d_e \neq 1$, separately.

HEE for $d_e = 1$

For the zero-cutoff case, one has [Dong, Harrison, Kachru, Torroba,Wang '12]

$$r_t = \frac{\ell}{2}.$$

Moreover, the HEE is given by

$$S_0 = \frac{R^d}{2G_N}\left(\frac{L}{r_F}\right)^{d-1}\log\left(\frac{\ell}{\epsilon}\right),$$

HEE for $d_e = 1$

For the zero-cutoff case, one has [Dong, Harrison, Kachru, Torroba,Wang '12]

$$r_t = \frac{\ell}{2}.$$

Moreover, the HEE is given by

$$S_0 = \frac{R^d}{2G_N}\left(\frac{L}{r_F}\right)^{d-1}\log\left(\frac{\ell}{\epsilon}\right),$$

For the finite-cutoff case when $d_e = 1$, one can find r_t and HEE exactly.

$$r_t = \sqrt{\left(\frac{\ell}{2}\right)^2 + r_c^2}.$$

$$S = \frac{R^d}{2G_N}\left(\frac{L}{r_F}\right)^{d-1}\log\left(\frac{\ell + \sqrt{\ell^2 + 4r_c^2}}{2r_c}\right).$$

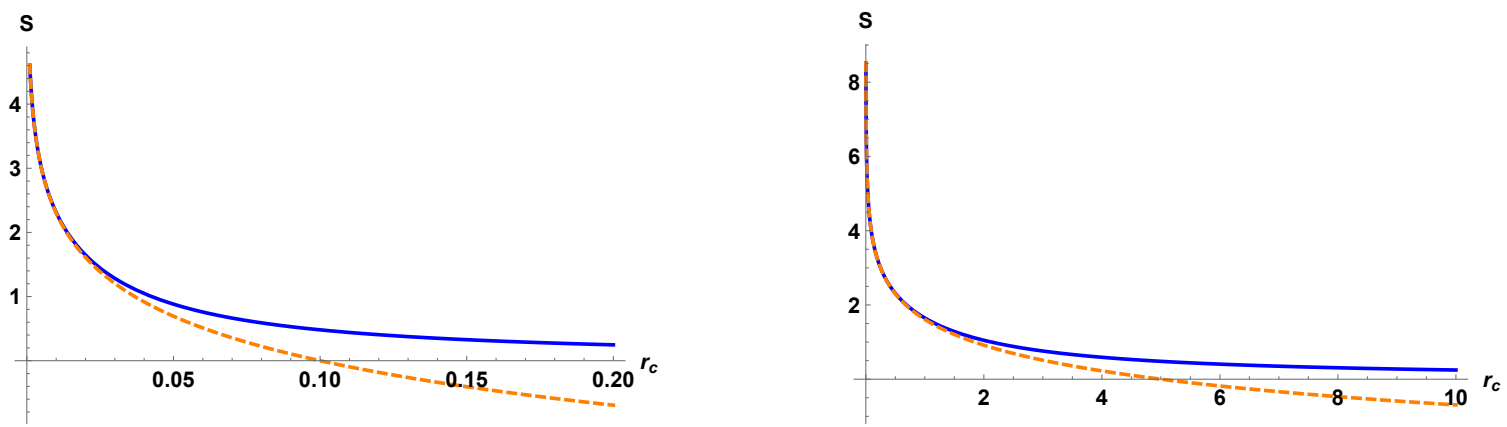

Figure: *Left*) $\ell = 0.1$ *Right*) $\ell = 5$.

HEE for $d_e \neq 1$

For the zero-cutoff case, one has

$$r_t = \frac{\ell}{2\Upsilon}, \qquad \Upsilon = \frac{\sqrt{\pi}\Gamma\left(\frac{d_e+1}{2d_e}\right)}{\Gamma\left(\frac{1}{2d_e}\right)}$$

In this case, the HEE is given by [Dong, Harrison, Kachru, Torroba,Wang '12]

$$S_0 = \frac{R^d L^{d-1}}{2G_N(d_e-1)r_F^\theta}\left[\frac{1}{\epsilon^{d_e-1}} - \Upsilon^{d_e}\left(\frac{2}{\ell}\right)^{d_e-1}\right].$$

HEE for $d_e \neq 1$

For the zero-cutoff case, one has

$$r_t = \frac{\ell}{2\Upsilon}, \qquad \Upsilon = \frac{\sqrt{\pi}\Gamma\left(\frac{d_e+1}{2d_e}\right)}{\Gamma\left(\frac{1}{2d_e}\right)}$$

In this case, the HEE is given by [Dong, Harrison, Kachru, Torroba,Wang '12]

$$S_0 = \frac{R^d L^{d-1}}{2G_N(d_e-1)r_F^\theta}\left[\frac{1}{\epsilon^{d_e-1}} - \Upsilon^{d_e}\left(\frac{2}{\ell}\right)^{d_e-1}\right].$$

For the finite cutoff case, one has

$$\frac{\ell}{2} = \Upsilon r_t - \frac{r_c^{d_e+1}}{(d_e+1)r_t^{d_e}}\ {}_2F_1\left[\frac{1}{2}, \frac{d_e+1}{2d_e}, \frac{3d_e+1}{2d_e}, \left(\frac{r_c}{r_t}\right)^{2d_e}\right],$$

HEE for $d_e \neq 1$

For the zero-cutoff case, one has

$$r_t = \frac{\ell}{2\Upsilon}, \qquad \Upsilon = \frac{\sqrt{\pi}\Gamma\left(\frac{d_e+1}{2d_e}\right)}{\Gamma\left(\frac{1}{2d_e}\right)}$$

In this case, the HEE is given by [Dong, Harrison, Kachru, Torroba,Wang '12]

$$S_0 = \frac{R^d L^{d-1}}{2G_N(d_e-1)r_F^\theta}\left[\frac{1}{\epsilon^{d_e-1}} - \Upsilon^{d_e}\left(\frac{2}{\ell}\right)^{d_e-1}\right].$$

For the finite cutoff case, one has

$$\frac{\ell}{2} = \Upsilon r_t - \frac{r_c^{d_e+1}}{(d_e+1)r_t^{d_e}}\ {}_2F_1\left[\frac{1}{2}, \frac{d_e+1}{2d_e}, \frac{3d_e+1}{2d_e}, \left(\frac{r_c}{r_t}\right)^{2d_e}\right],$$

$$S = \frac{R^d L^{d-1}}{2G_N r_F^\theta(d_e-1)}\left[-\frac{\Upsilon}{r_t^{d_e-1}} + \frac{1}{r_c^{d_e-1}}\ {}_2F_1\left[\frac{1}{2}, \frac{1-d_e}{2d_e}, \frac{d_e+1}{2d_e}, \left(\frac{r_c}{r_t}\right)^{2d_e}\right]\right].$$

HEE for $d_e \neq 1$

For the zero-cutoff case, one has

$$r_t = \frac{\ell}{2\Upsilon}, \qquad \Upsilon = \frac{\sqrt{\pi}\Gamma\left(\frac{d_e+1}{2d_e}\right)}{\Gamma\left(\frac{1}{2d_e}\right)}$$

In this case, the HEE is given by [Dong, Harrison, Kachru, Torroba,Wang '12]

$$S_0 = \frac{R^d L^{d-1}}{2G_N(d_e-1)r_F^\theta}\left[\frac{1}{\epsilon^{d_e-1}} - \Upsilon^{d_e}\left(\frac{2}{\ell}\right)^{d_e-1}\right].$$

For the finite cutoff case, one has

$$\frac{\ell}{2} = \Upsilon r_t - \frac{r_c^{d_e+1}}{(d_e+1)r_t^{d_e}}\ {}_2F_1\left[\frac{1}{2}, \frac{d_e+1}{2d_e}, \frac{3d_e+1}{2d_e}, \left(\frac{r_c}{r_t}\right)^{2d_e}\right],$$

$$S = \frac{R^d L^{d-1}}{2G_N r_F^\theta(d_e-1)}\left[-\frac{\Upsilon}{r_t^{d_e-1}} + \frac{1}{r_c^{d_e-1}}\ {}_2F_1\left[\frac{1}{2}, \frac{1-d_e}{2d_e}, \frac{d_e+1}{2d_e}, \left(\frac{r_c}{r_t}\right)^{2d_e}\right]\right].$$

Therefore, one cannot find analytic expressions for r_t and S. We calculate them numerically and perturbatively for

- Very small entangling region: $r_t \approx r_c \gg \ell$
- Very large entangling region: $\ell \approx r_t \gg r_c$

For very large entangling region, one has $S = S_0 + \Delta S$ where

$$\Delta S = \frac{R^d L^{d-1}}{4 G_N r_F^\theta (d_e+1)} \left(\frac{2\Upsilon}{\ell}\right)^{2d_e} \Big[r_c^{d_e+1} - \frac{3(d_e+1)}{4(3d_e+1)} \left(\frac{2\Upsilon}{\ell}\right)^{2d_e} r_c^{3d_e+1} - \frac{d_e(3d_e+1)}{3(d_e+1)^2\Upsilon} \left(\frac{2\Upsilon}{\ell}\right)^{2(d_e+1)} r_c^{3(d_e+1)} + \cdots \Big].$$

For very small entangling regions, one obtains

$$S = \frac{R^d L^{d-1}}{4 G_N r_F^\theta} \frac{1}{r_c^{d_e-1}} \Big[\left(\frac{\ell}{r_c}\right) - \frac{d_e^2}{24} \left(\frac{\ell}{r_c}\right)^3 + \frac{d_e^2\,(4d_e(39+5d_e)-47)}{30720} \left(\frac{\ell}{r_c}\right)^5 + \frac{d_e^3(5071 - 4d_e(2561+113d_e))}{10321920} \left(\frac{\ell}{r_c}\right)^7 + \cdots \Big].$$

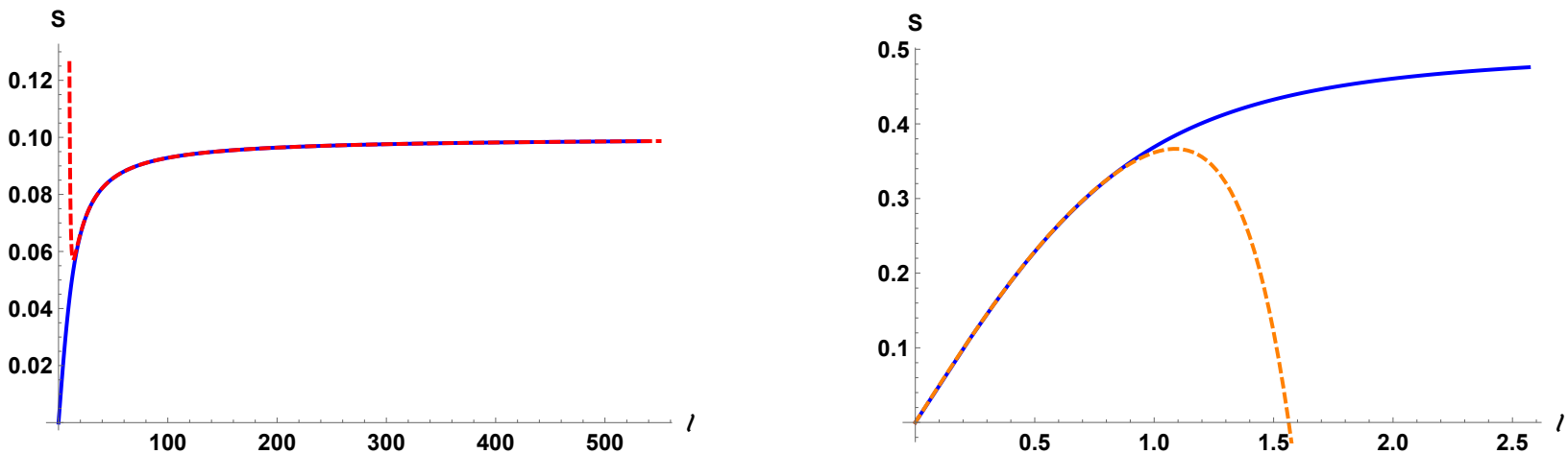

Figure: *Left*) $r_c = 10$ and $d_e = 2$. *right*) $r_c = 1$ and $d_e = 3$.

HMI for $d_e = 1$

For the zero-cutoff case, one has [Fischler, Kundu, '12]

$$I_0(A,B) = \begin{cases} 0 & \ell \ll h \\ \frac{R^d L^{d-1}}{2 G_N r_F^\theta} \log\left(\frac{\ell^2}{h(2\ell+h)}\right) & \ell \gg h \end{cases}$$

which is independent of the UV cutoff and when $h \to 0$, one has $I_0 \to \infty$.

HMI for $d_e = 1$

For the zero-cutoff case, one has [Fischler, Kundu, '12]

$$I_0(A,B) = \begin{cases} 0 & \ell \ll h \\ \frac{R^d L^{d-1}}{2 G_N r_F^\theta} \log\left(\frac{\ell^2}{h(2\ell+h)}\right) & \ell \gg h \end{cases}$$

which is independent of the UV cutoff and when $h \to 0$, one has $I_0 \to \infty$.
Moreover, there is a first-order phase transition at

$$h^{(0)}_{\text{crit.}} = \ell(\sqrt{2}-1).$$

It is also independent of the UV cutoff.

HMI for $d_e = 1$

For the zero-cutoff case, one has [Fischler, Kundu, '12]

$$I_0(A,B) = \begin{cases} 0 & \ell \ll h \\ \frac{R^d L^{d-1}}{2 G_N r_F^\theta} \log\left(\frac{\ell^2}{h(2\ell+h)}\right) & \ell \gg h \end{cases}$$

which is independent of the UV cutoff and when $h \to 0$, one has $I_0 \to \infty$.
Moreover, there is a first-order phase transition at

$$h^{(0)}_{\text{crit.}} = \ell(\sqrt{2}-1).$$

It is also independent of the UV cutoff.
For the finite cutoff case, one can find analytic expressions for the HMI

$$I(A,B) = \begin{cases} 0 & \ell \ll h \\ \frac{R^d L^{d-1}}{2 G_N r_F^{d-1}} \log\left(\frac{\left(\ell+\sqrt{\ell^2+4r_c^2}\right)^2}{\left(h+\sqrt{h^2+4r_c^2}\right)\left((2\ell+h)+\sqrt{(2\ell+h)^2+4r_c^2}\right)}\right) & \ell \gg h \end{cases}$$

HMI for $d_e = 1$

For the zero-cutoff case, one has [Fischler, Kundu, '12]

$$I_0(A,B) = \begin{cases} 0 & \ell \ll h \\ \frac{R^d L^{d-1}}{2 G_N r_F^\theta} \log\left(\frac{\ell^2}{h(2\ell+h)}\right) & \ell \gg h \end{cases}$$

which is independent of the UV cutoff and when $h \to 0$, one has $I_0 \to \infty$.
Moreover, there is a first-order phase transition at

$$h^{(0)}_{\text{crit.}} = \ell(\sqrt{2}-1).$$

It is also independent of the UV cutoff.
For the finite cutoff case, one can find analytic expressions for the HMI

$$I(A,B) = \begin{cases} 0 & \ell \ll h \\ \frac{R^d L^{d-1}}{2 G_N r_F^{d-1}} \log\left(\frac{\left(\ell+\sqrt{\ell^2+4r_c^2}\right)^2}{\left(h+\sqrt{h^2+4r_c^2}\right)\left((2\ell+h)+\sqrt{(2\ell+h)^2+4r_c^2}\right)}\right) & \ell \gg h \end{cases}$$

$$h_{\text{crit.}} = \ell\left(-1 + \frac{\sqrt{2}(\ell^2+2r_c^2)}{\sqrt{\ell^4+6\ell^2 r_c^2+8r_c^4}}\right).$$

which depends on r_c.

HMI for $d_e = 1$

For the zero-cutoff case, one has [Fischler, Kundu, '12]

$$I_0(A,B) = \begin{cases} 0 & \ell \ll h \\ \frac{R^d L^{d-1}}{2G_N r_F^\theta} \log\left(\frac{\ell^2}{h(2\ell+h)}\right) & \ell \gg h \end{cases}$$

which is independent of the UV cutoff and when $h \to 0$, one has $I_0 \to \infty$.
Moreover, there is a first-order phase transition at

$$h^{(0)}_{\text{crit.}} = \ell(\sqrt{2}-1).$$

It is also independent of the UV cutoff.
For the finite cutoff case, one can find analytic expressions for the HMI

$$I(A,B) = \begin{cases} 0 & \ell \ll h \\ \frac{R^d L^{d-1}}{2G_N r_F^{d-1}} \log\left(\frac{\left(\ell+\sqrt{\ell^2+4r_c^2}\right)^2}{\left(h+\sqrt{h^2+4r_c^2}\right)\left((2\ell+h)+\sqrt{(2\ell+h)^2+4r_c^2}\right)}\right) & \ell \gg h \end{cases}$$

$$h_{\text{crit.}} = \ell\left(-1+\frac{\sqrt{2}(\ell^2+2r_c^2)}{\sqrt{\ell^4+6\ell^2 r_c^2+8r_c^4}}\right).$$

which depends on r_c.
Moreover, when $h \to 0$, HMI is finite

$$I(A,B) = \frac{R^d L^{d-1}}{2G_N r_F^{d-1}} \log\left(\frac{\left(\ell+\sqrt{\ell^2+4r_c^2}\right)^2}{r_c\left(\ell+\sqrt{\ell^2+r_c^2}\right)}\right).$$

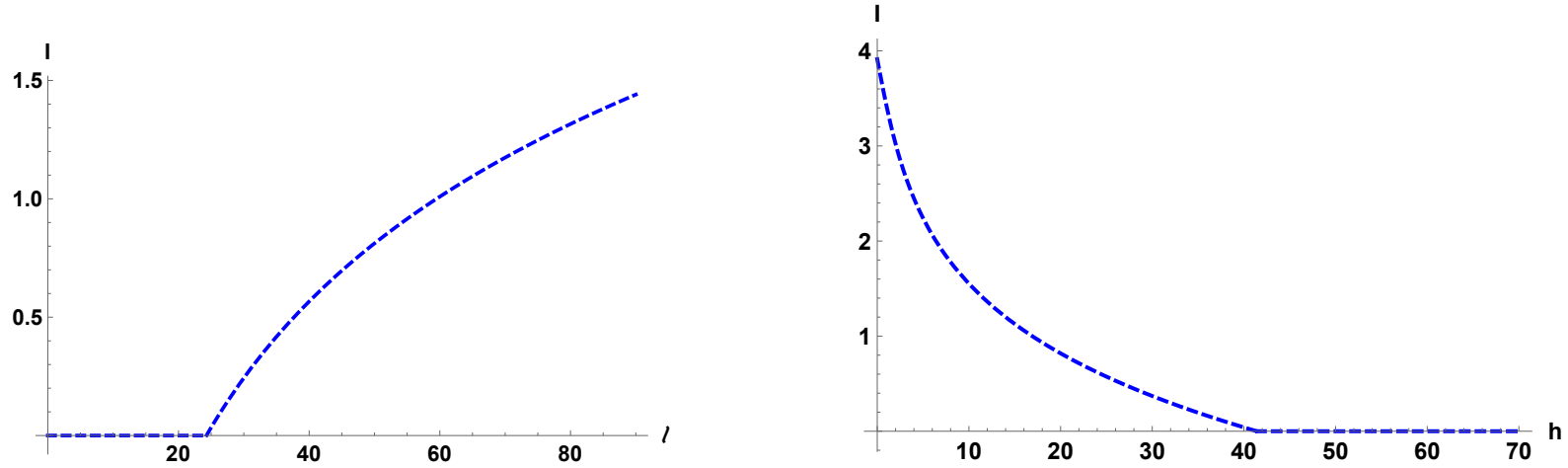

Figure: *Left*) $r_c = 1$ and $h = 10$. *Right*) $r_c = 1$ and $\ell = 100$.

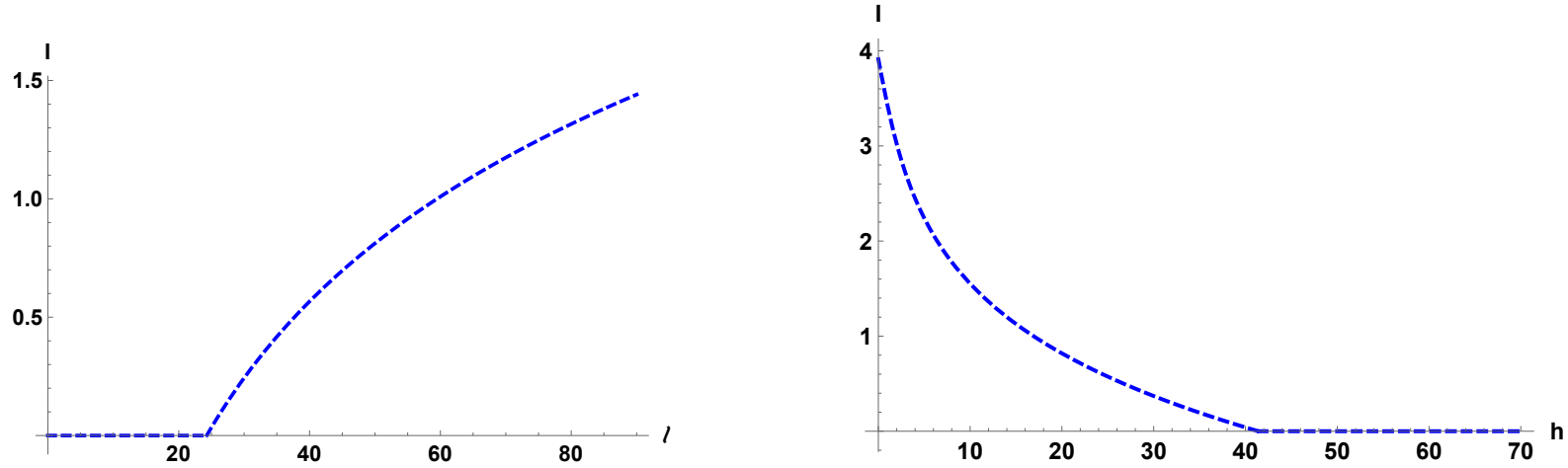

Figure: *Left*) $r_c = 1$ and $h = 10$. *Right*) $r_c = 1$ and $\ell = 100$.

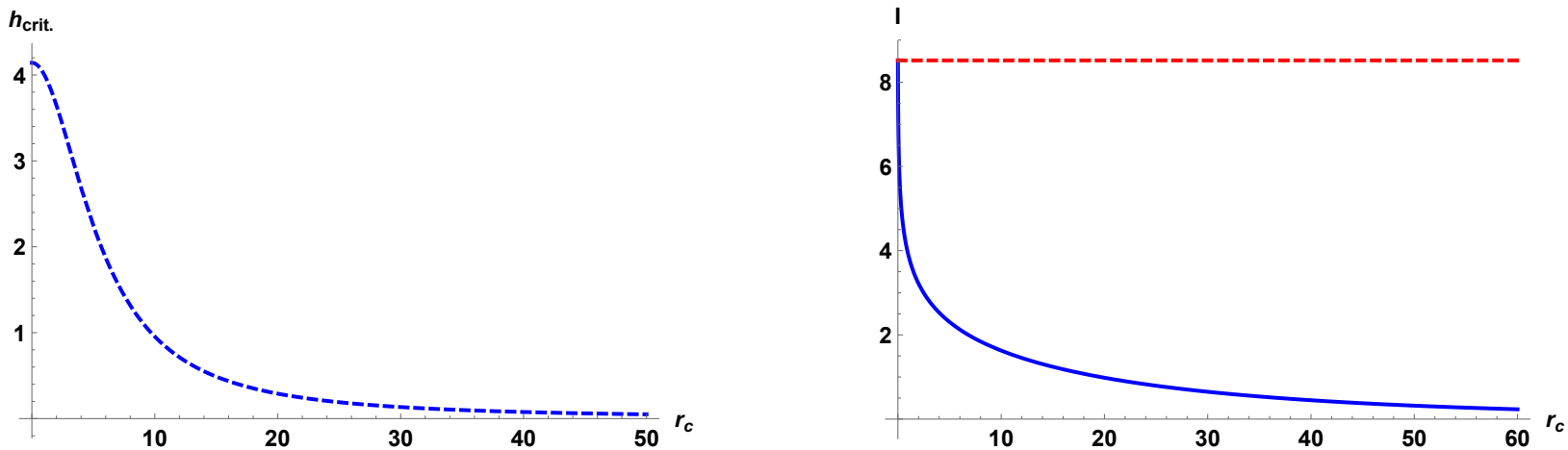

Figure: *Left*) $\ell = 10$. *Right*) $l = 10^2$, $h = 10^{-2}$.

$h_{\text{crit.}}$ and the HMI are decreasing functions of r_c.

HMI for $d_e \neq 1$

In this case. one can only calculate the HMI numerically or perturbatively for very large or small entangling regions.

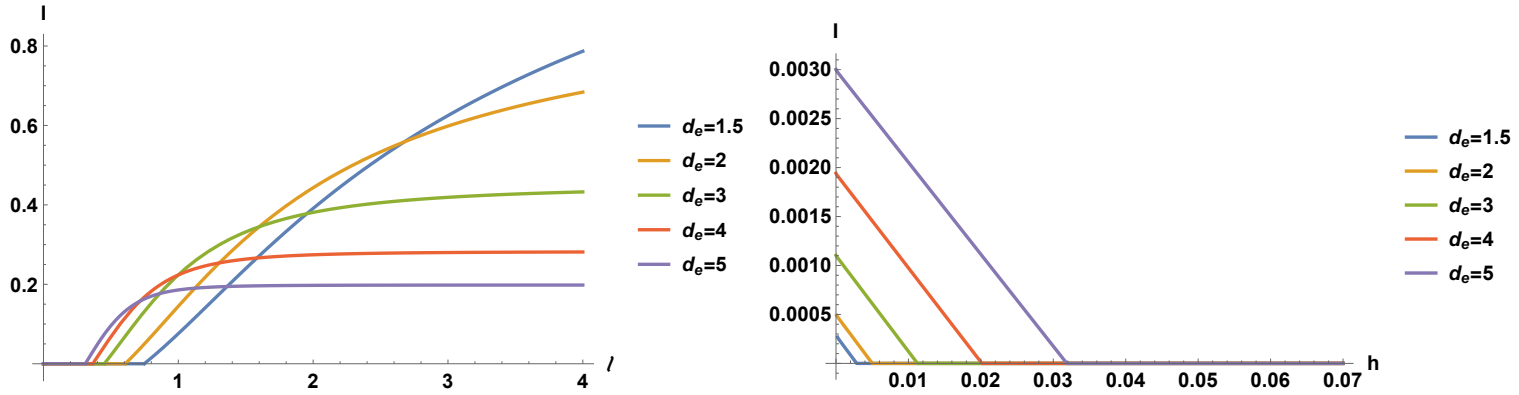

Figure: *Left*) $h = 0.1$ and $r_c = 1$. *Right*) $\ell = 1$ and $r_c = 10$.

HMI for $d_e \neq 1$

In this case. one can only calculate the HMI numerically or perturbatively for very large or small entangling regions.

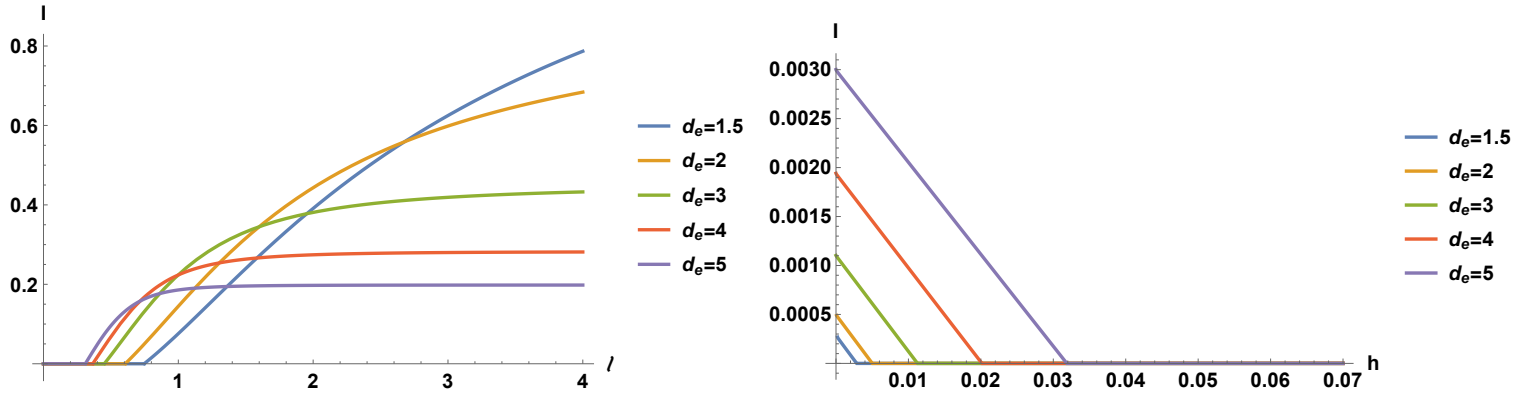

Figure: *Left*) $h = 0.1$ and $r_c = 1$. *Right*) $\ell = 1$ and $r_c = 10$.

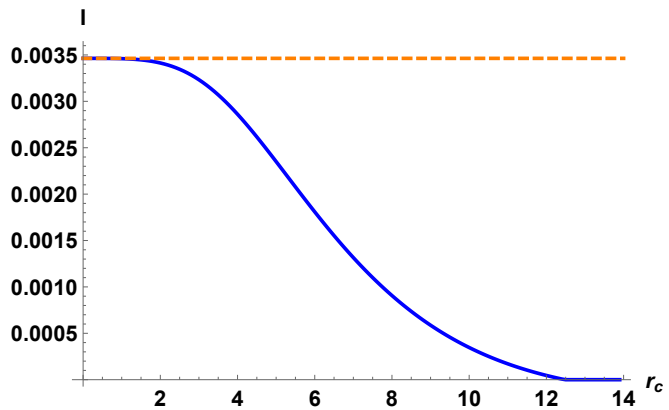

Figure: $\ell = 10$, $h = 5$ and $d_e = 3$.

It is a decreasing function of r_c.

HMI for Very Large ER: $\ell \gg r_c$

$$I(A,B) = \begin{cases} 0 & \ell \ll h \\ I_0 + \Delta I & \ell \gg h \end{cases}$$

where [Fischler, Kundu, '12]

$$I_0 = -\frac{R^d L^{d-1}}{2 G_N r_F^\theta (d_e - 1)} \Upsilon^{d_e} \mathcal{I}(d_e - 1),$$

$$\mathcal{I}(n) = 2\left(\frac{2}{\ell}\right)^n - \left(\frac{2}{h}\right)^n - \left(\frac{2}{2\ell + h}\right)^n.$$

I_0 is independent of the cutoff r_c. Moreover, it goes to infinity when $h \to 0$.

HMI for Very Large ER: $\ell \gg r_c$

$$I(A,B) = \begin{cases} 0 & \ell \ll h \\ I_0 + \Delta I & \ell \gg h \end{cases}$$

where [Fischler, Kundu, '12]

$$I_0 = -\frac{R^d L^{d-1}}{2G_N r_F^\theta (d_e - 1)} \Upsilon^{d_e}\, \mathcal{I}(d_e - 1),$$

$$\mathcal{I}(n) = 2\left(\frac{2}{\ell}\right)^n - \left(\frac{2}{h}\right)^n - \left(\frac{2}{2\ell + h}\right)^n.$$

I_0 is independent of the cutoff r_c. Moreover, it goes to infinity when $h \to 0$.

$$\Delta I = \frac{R^d L^{d-1}}{4G_N r_F^\theta (d_e + 1)} \Upsilon^{2d_e}\, r_c^{d_e+1} \left[\mathcal{I}(2d_e) - \frac{3(d_e+1)}{4(3de+1)}\, \mathcal{I}(4d_e)\, (\Upsilon r_c)^{2d_e} - \frac{d_e(3d_e+1)}{3(d_e+1)^2 \Upsilon}\, \mathcal{I}(4d_e+2)\, (\Upsilon r_c)^{2(d_e+1)} + \cdots\right].$$

HMI for Very Large ER: $\ell \gg r_c$

$$I(A,B) = \begin{cases} 0 & \ell \ll h \\ I_0 + \Delta I & \ell \gg h \end{cases}$$

where [Fischler, Kundu, '12]

$$I_0 = -\frac{R^d L^{d-1}}{2 G_N r_F^\theta (d_e - 1)} \Upsilon^{d_e}\, \mathcal{I}(d_e - 1),$$

$$\mathcal{I}(n) = 2\left(\frac{2}{\ell}\right)^n - \left(\frac{2}{h}\right)^n - \left(\frac{2}{2\ell + h}\right)^n.$$

I_0 is independent of the cutoff r_c. Moreover, it goes to infinity when $h \to 0$.

$$\Delta I = \frac{R^d L^{d-1}}{4 G_N r_F^\theta (d_e + 1)} \Upsilon^{2d_e}\, r_c^{d_e+1} \left[\mathcal{I}(2d_e) - \frac{3(d_e+1)}{4(3de+1)}\, \mathcal{I}(4d_e)\, (\Upsilon r_c)^{2d_e} \right.$$
$$\left. - \frac{d_e(3d_e+1)}{3(d_e+1)^2 \Upsilon}\, \mathcal{I}(4d_e+2)\, (\Upsilon r_c)^{2(d_e+1)} + \cdots \right].$$

For $d_e = 2$, one has

$$h_{\text{crit.}} = h^{(0)}_{\text{crit.}} + \ell \left[-0.844 \left(\frac{r_c}{\ell}\right)^3 - 5.38 \left(\frac{r_c}{\ell}\right)^6 \right.$$
$$\left. + 5.16 \left(\frac{r_c}{\ell}\right)^7 + 5.74 \left(\frac{r_c}{\ell}\right)^9 - 88.0 \left(\frac{r_c}{\ell}\right)^{10} + \cdots \right],$$

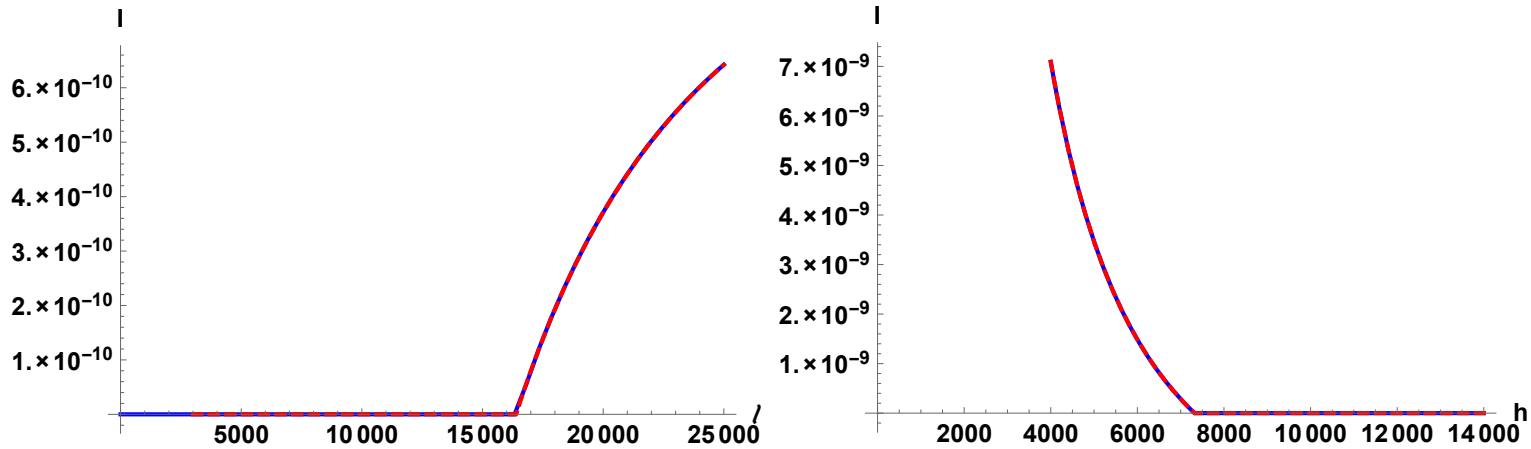

Figure: *Left*) $h = 1.2 \times 10^4$, $r_c = 1$ and $d_e = 3$. *Right*) $\ell = 10^4$, $r_c = 1$ and $d_e = 3$.

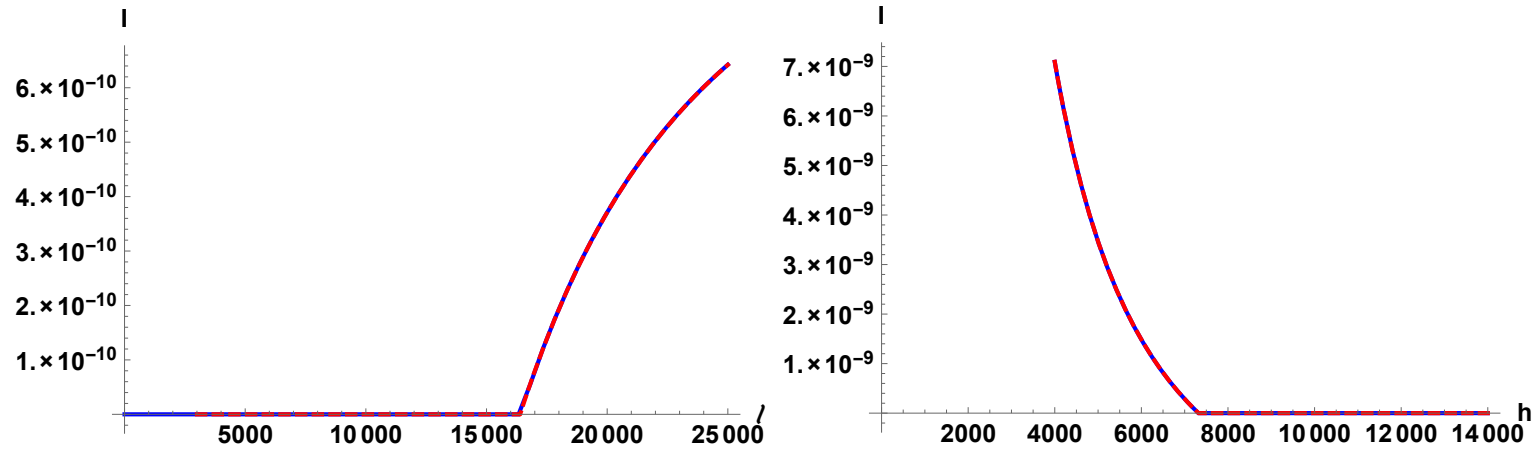

Figure: *Left)* $h = 1.2 \times 10^4$, $r_c = 1$ and $d_e = 3$. *Right)* $\ell = 10^4$, $r_c = 1$ and $d_e = 3$.

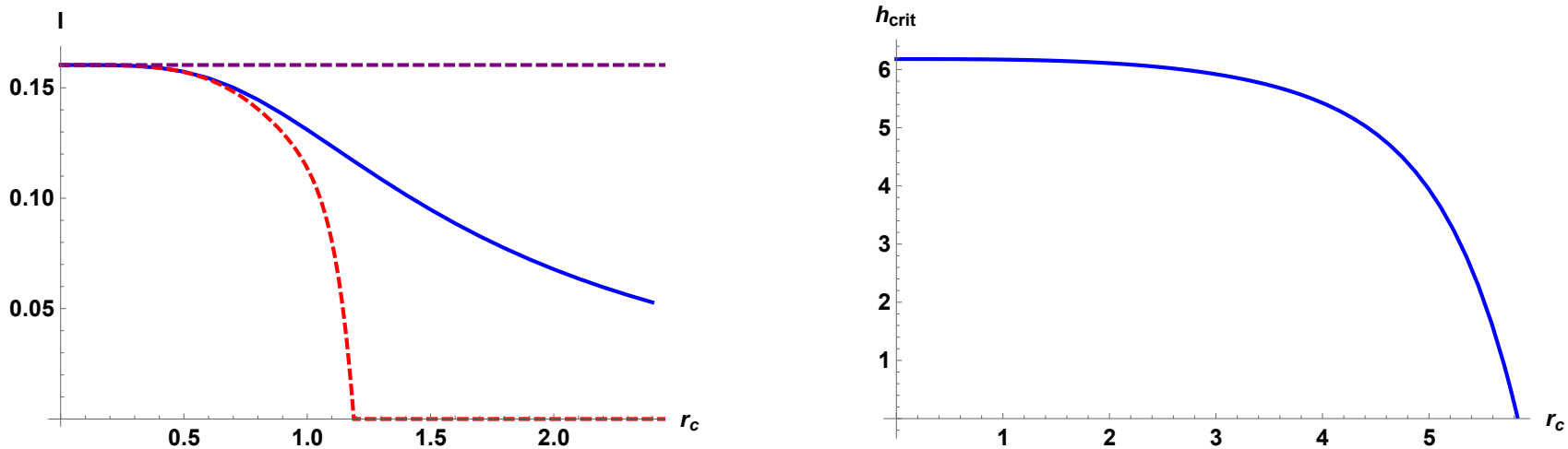

Figure: *Left)* $l = 10^4$, $h = 1$ and $d_e = 3$. *Right)* $\ell = 10$ and $d_e = 2$.

$h_{\text{crit.}}$ is a decreasing function of r_c.

HMI for Very Small ER: $\ell \ll r_c$,

$$I(A,B) = \begin{cases} 0 & \ell \ll h \\ I_s & \ell \gg h \end{cases}$$

where

$$I_s = \frac{R^d L^{d-1}}{4 G_N r_F^\theta} \frac{d_e^2}{r_c^{d_e-1}} \left[-\frac{1}{24}\frac{\mathcal{K}(3)}{r_c^3} + \frac{(4d_e(39+5d_e)-47)}{30720}\frac{\mathcal{K}(5)}{r_c^5} + \frac{d_e(5071-4d_e(2561+113d_e))}{10321920}\frac{\mathcal{K}(7)}{r_c^7} + \cdots \right],$$

and $\mathcal{K}(n)$ is defined as follows

$$\mathcal{K}(n) = 2\ell^n - (2\ell + h)^n - h^n.$$

HMI for Very Small ER: $\ell \ll r_c$,

$$I(A,B) = \begin{cases} 0 & \ell \ll h \\ I_s & \ell \gg h \end{cases}$$

where

$$I_s = \frac{R^d L^{d-1}}{4 G_N r_F^\theta} \frac{d_e^2}{r_c^{d_e-1}} \left[-\frac{1}{24}\frac{\mathcal{K}(3)}{r_c^3} + \frac{(4d_e(39+5d_e)-47)}{30720}\frac{\mathcal{K}(5)}{r_c^5} + \frac{d_e(5071-4d_e(2561+113d_e))}{10321920}\frac{\mathcal{K}(7)}{r_c^7} + \cdots \right],$$

and $\mathcal{K}(n)$ is defined as follows

$$\mathcal{K}(n) = 2\ell^n - (2\ell+h)^n - h^n.$$

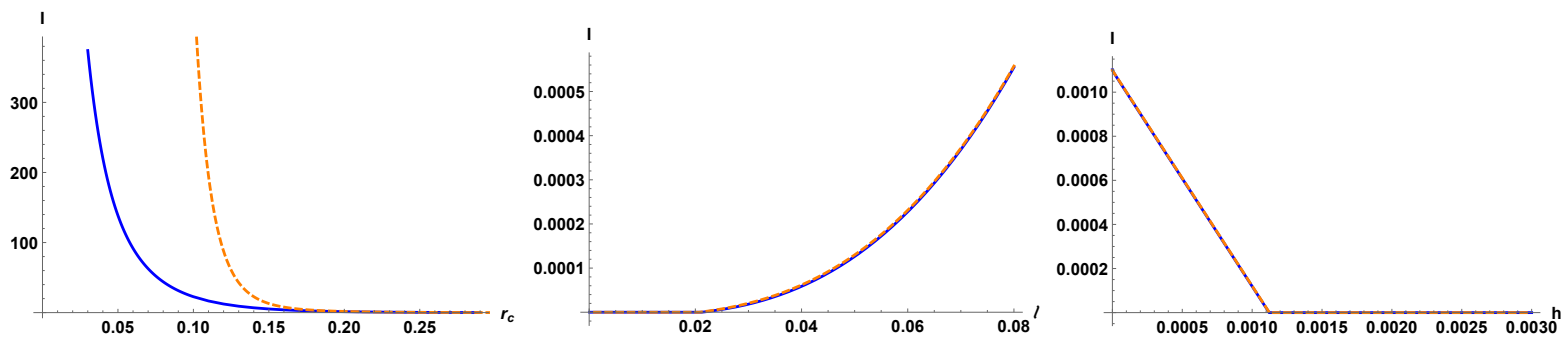

Figure: *Left)* $h = 10^{-2}$, $\ell = 10^{-1}$ and $d_e = 3$. *Middle)* $h = 10^{-5}$, $r_c = 1$ *Right)* $\ell = 0.1$, $r_c = 1$

We calculate the EWCS for two parallel strips with equal widths ℓ which are separated by the distance h.

$$E_W = \frac{R^d L^{d-1}}{4 G_N r_F^\theta} \int_{r_t(h)}^{r_t(2\ell+h)} \frac{dr}{r^{d_e}},$$

We calculate the EWCS for two parallel strips with equal widths ℓ which are separated by the distance h.

$$E_W = \frac{R^d L^{d-1}}{4 G_N r_F^\theta} \int_{r_t(h)}^{r_t(2\ell+h)} \frac{dr}{r^{d_e}},$$

when the strips are far enough from each other, the EW is disconnected. In this case, there is no minimal surface $\Sigma_{AB}^{\min}$, and hence $E_W = 0$.

We calculate the EWCS for two parallel strips with equal widths ℓ which are separated by the distance h.

$$E_W = \frac{R^d L^{d-1}}{4 G_N r_F^\theta} \int_{r_t(h)}^{r_t(2\ell+h)} \frac{dr}{r^{d_e}},$$

when the strips are far enough from each other, the EW is disconnected. In this case, there is no minimal surface $\Sigma_{AB}^{\min}$, and hence $E_W = 0$.
For $d_e = 1$ and the zero cutoff case, one obtains

$$E_W^0 = \frac{R^d L^{d-1}}{4 G_N r_F^\theta} \log\left(\frac{2\ell + h}{h}\right),$$

We calculate the EWCS for two parallel strips with equal widths ℓ which are separated by the distance h.

$$E_W = \frac{R^d L^{d-1}}{4 G_N r_F^\theta} \int_{r_t(h)}^{r_t(2\ell+h)} \frac{dr}{r^{d_e}},$$

when the strips are far enough from each other, the EW is disconnected. In this case, there is no minimal surface $\Sigma_{AB}^{\min}$, and hence $E_W = 0$.
For $d_e = 1$ and the zero cutoff case, one obtains

$$E_W^0 = \frac{R^d L^{d-1}}{4 G_N r_F^\theta} \log\left(\frac{2\ell + h}{h}\right),$$

For $d_e = 1$ and the finite cutoff case, one has

$$E_W = \frac{R^d L^{d-1}}{8 G_N r_F^\theta} \log\left(\frac{(2\ell + h)^2 + 4r_c^2}{h^2 + 4r_c^2}\right).$$

We calculate the EWCS for two parallel strips with equal widths ℓ which are separated by the distance h.

$$E_W = \frac{R^d L^{d-1}}{4 G_N r_F^\theta} \int_{r_t(h)}^{r_t(2\ell+h)} \frac{dr}{r^{d_e}},$$

when the strips are far enough from each other, the EW is disconnected. In this case, there is no minimal surface $\Sigma_{AB}^{\min}$, and hence $E_W = 0$.
For $d_e = 1$ and the zero cutoff case, one obtains

$$E_W^0 = \frac{R^d L^{d-1}}{4 G_N r_F^\theta} \log\left(\frac{2\ell + h}{h}\right),$$

For $d_e = 1$ and the finite cutoff case, one has

$$E_W = \frac{R^d L^{d-1}}{8 G_N r_F^\theta} \log\left(\frac{(2\ell + h)^2 + 4r_c^2}{h^2 + 4r_c^2}\right).$$

- E_W depends on the cutoff r_c.

We calculate the EWCS for two parallel strips with equal widths ℓ which are separated by the distance h.

$$E_W = \frac{R^d L^{d-1}}{4 G_N r_F^\theta} \int_{r_t(h)}^{r_t(2\ell+h)} \frac{dr}{r^{d_e}},$$

when the strips are far enough from each other, the EW is disconnected. In this case, there is no minimal surface $\Sigma_{AB}^{\min}$, and hence $E_W = 0$.
For $d_e = 1$ and the zero cutoff case, one obtains

$$E_W^0 = \frac{R^d L^{d-1}}{4 G_N r_F^\theta} \log\left(\frac{2\ell + h}{h}\right),$$

For $d_e = 1$ and the finite cutoff case, one has

$$E_W = \frac{R^d L^{d-1}}{8 G_N r_F^\theta} \log\left(\frac{(2\ell + h)^2 + 4r_c^2}{h^2 + 4r_c^2}\right).$$

- E_W depends on the cutoff r_c.
- E_W is independent of the dynamical exponent z and depends on the hyperscaling violation exponent θ.

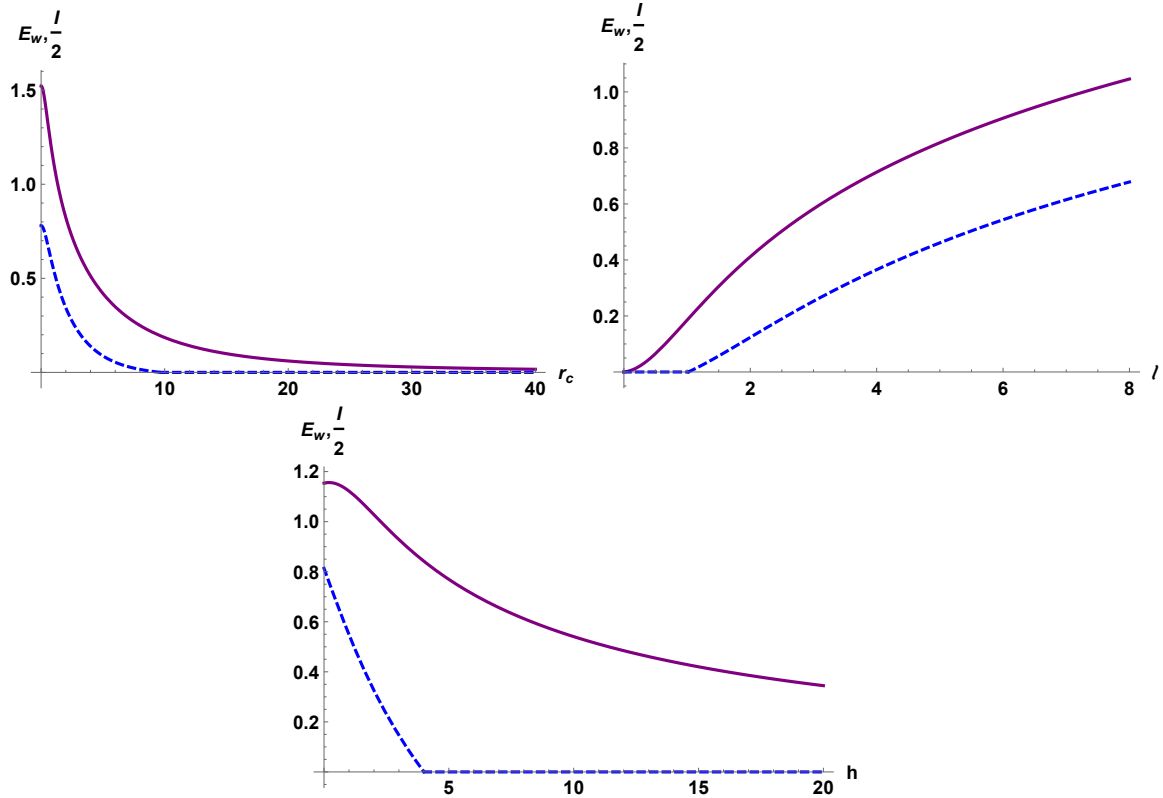

Figure: *Left*) $l = 10$ and $h = 1$. *Right*) $h = 0.1$ and $r_c = 1$. *Down*) $\ell = 10$ and $r_c = 1$.

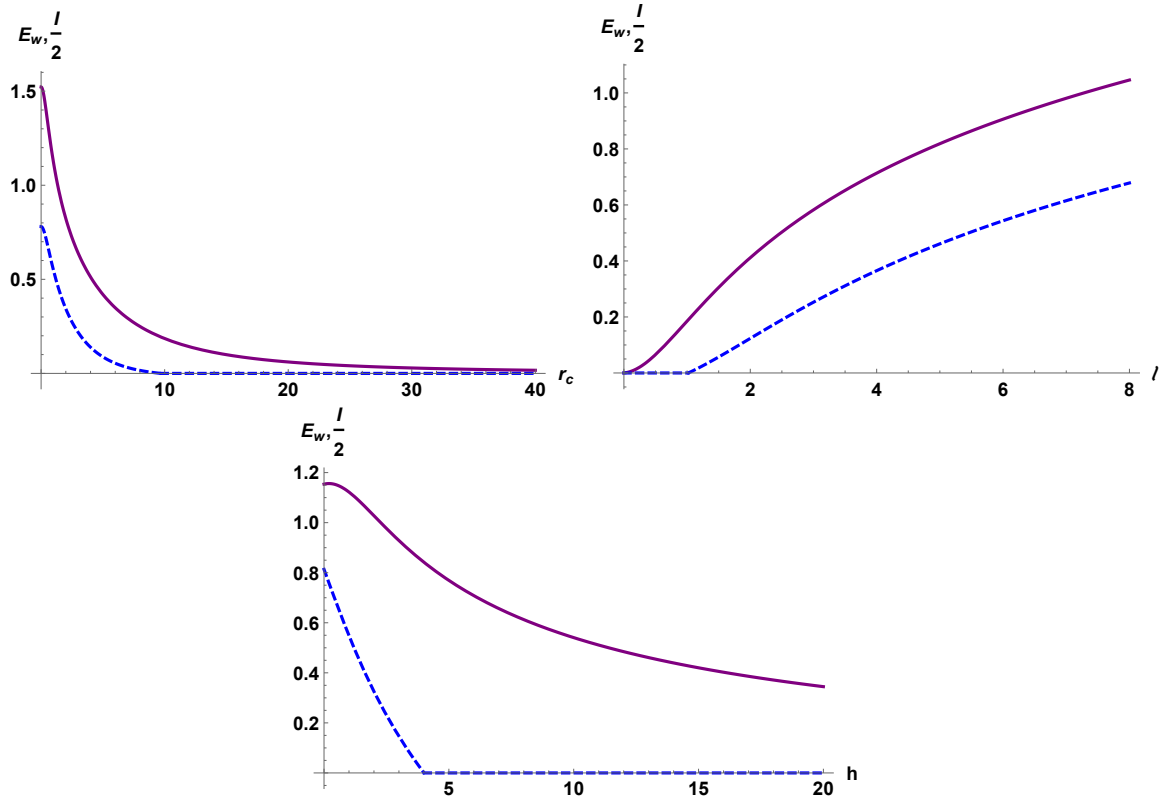

Figure: *Left*) $l = 10$ and $h = 1$. *Right*) $h = 0.1$ and $r_c = 1$. *Down*) $\ell = 10$ and $r_c = 1$.

- where the HMI undergoes a first-order phase transition, E_W is smooth and its concavity changes.

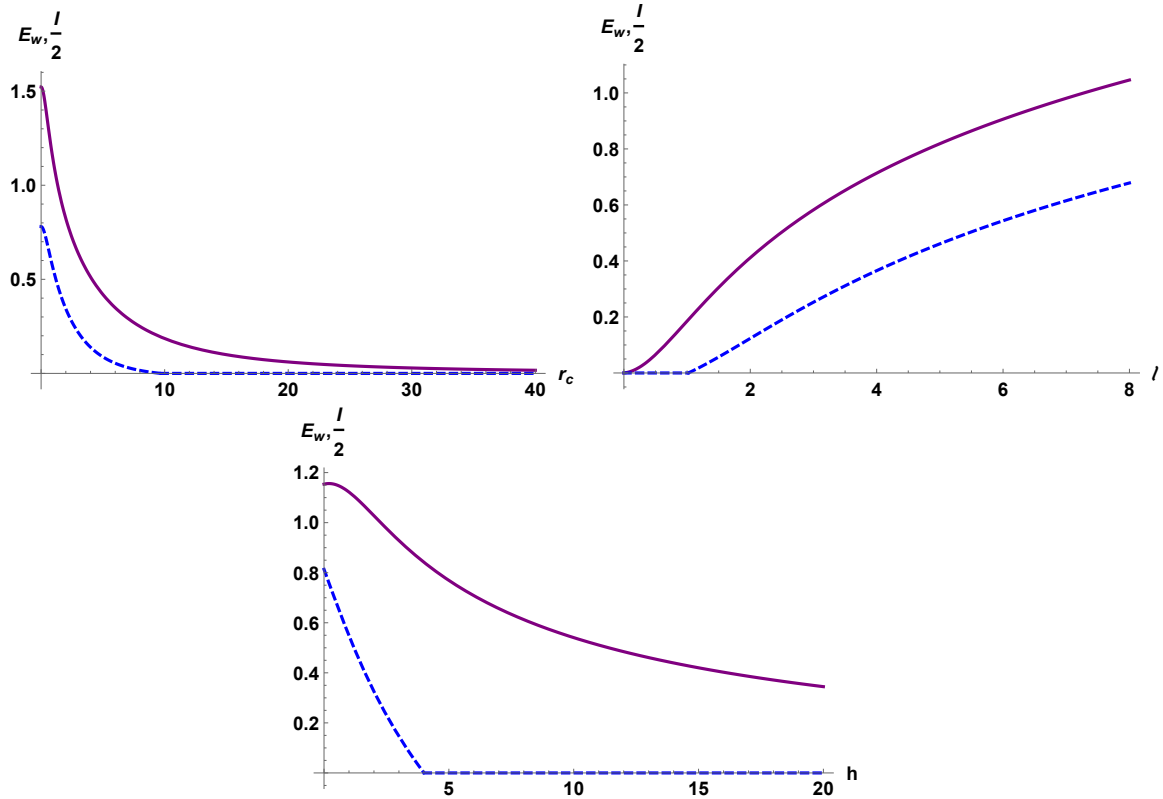

Figure: *Left*) $l = 10$ and $h = 1$. *Right*) $h = 0.1$ and $r_c = 1$. *Down*) $\ell = 10$ and $r_c = 1$.

- where the HMI undergoes a first-order phase transition, E_W is smooth and its concavity changes.
- similar to the zero cutoff case, by increasing the distance h, $E_W \to 0$.

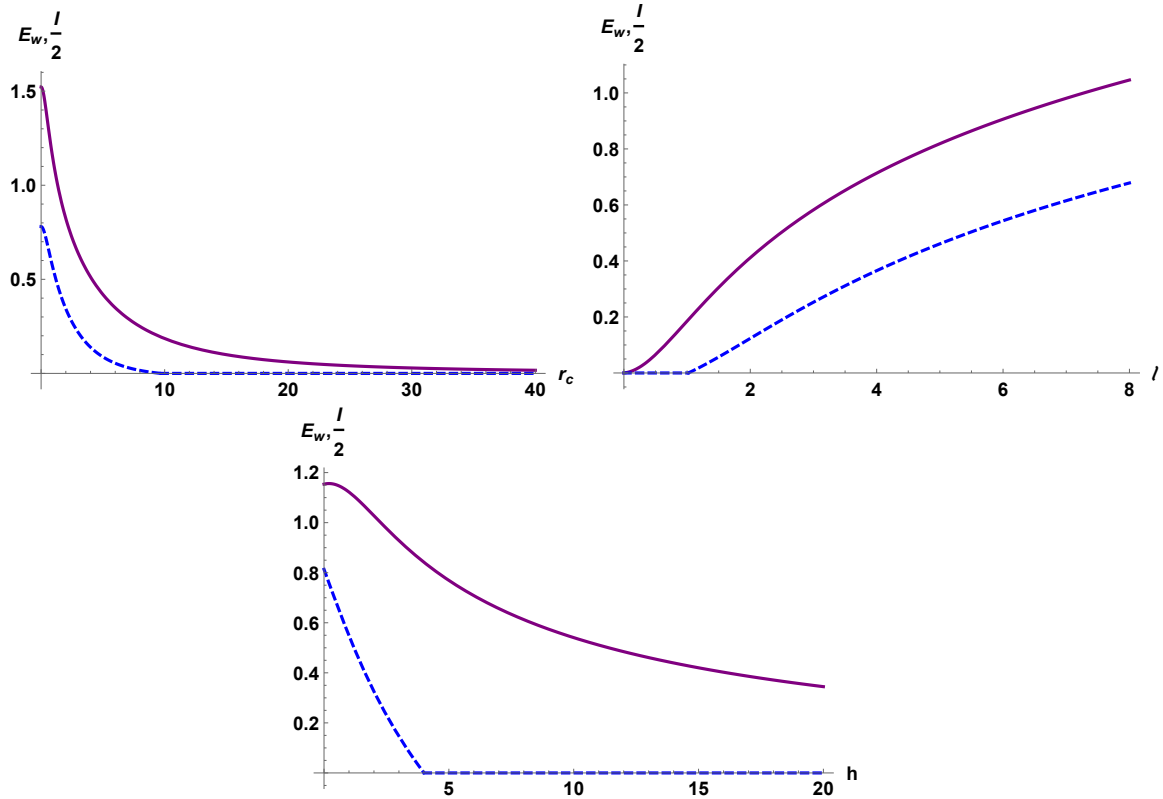

Figure: *Left*) $l = 10$ and $h = 1$. *Right*) $h = 0.1$ and $r_c = 1$. *Down*) $\ell = 10$ and $r_c = 1$.

- where the HMI undergoes a first-order phase transition, E_W is smooth and its concavity changes.
- similar to the zero cutoff case, by increasing the distance h, $E_W \to 0$.
- in the limit $h \to 0$, E_W^0 diverges. However, E_W remains finite in this limit.

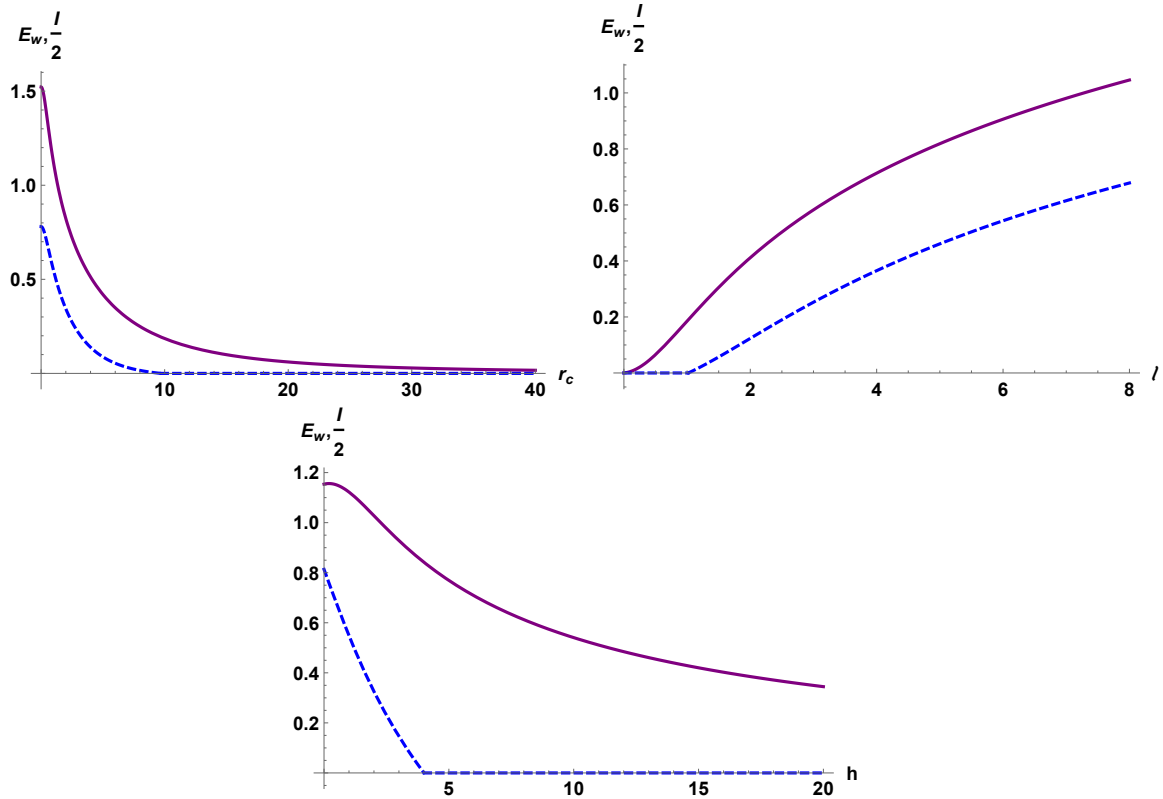

Figure: *Left*) $l = 10$ and $h = 1$. *Right*) $h = 0.1$ and $r_c = 1$. *Down*) $\ell = 10$ and $r_c = 1$.

- where the HMI undergoes a first-order phase transition, E_W is smooth and its concavity changes.
- similar to the zero cutoff case, by increasing the distance h, $E_W \to 0$.
- in the limit $h \to 0$, E_W^0 diverges. However, E_W remains finite in this limit.
- in the limit $h \to \infty$, E_W becomes zero which has the same behavior as in the zero cutoff case.

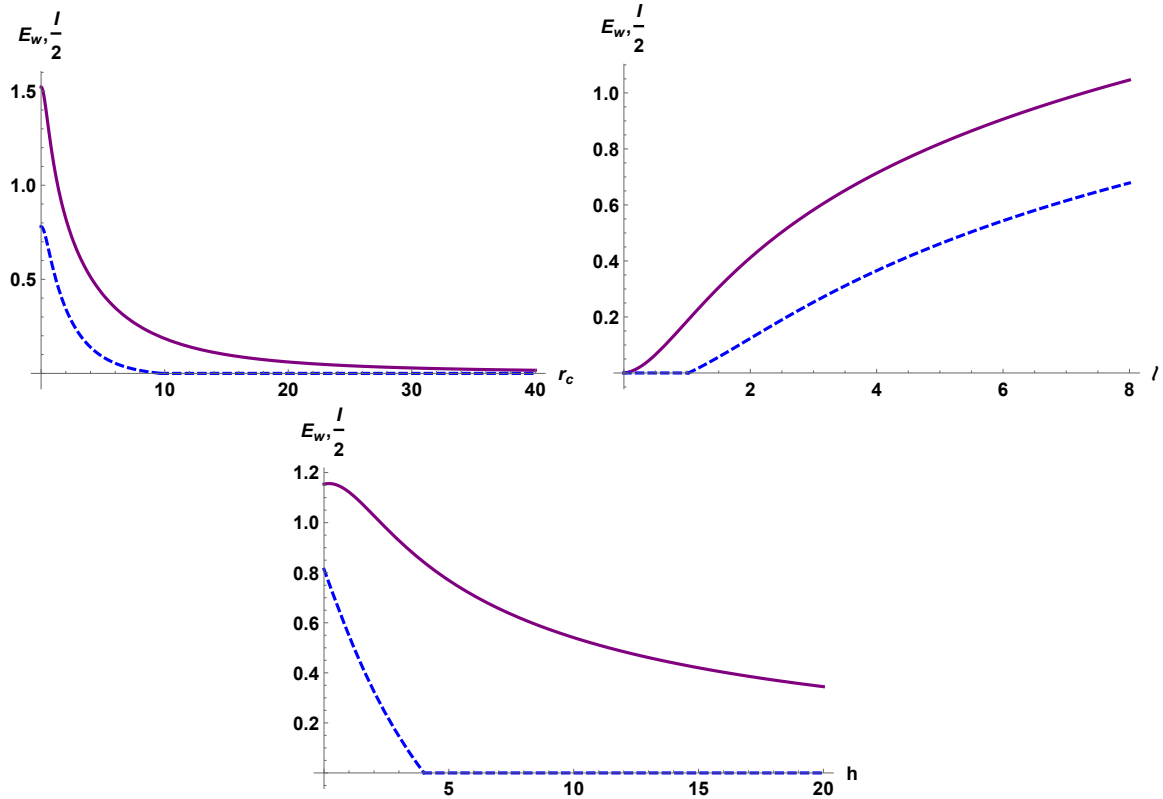

Figure: *Left*) $l = 10$ and $h = 1$. *Right*) $h = 0.1$ and $r_c = 1$. *Down*) $\ell = 10$ and $r_c = 1$.

- where the HMI undergoes a first-order phase transition, E_W is smooth and its concavity changes.
- similar to the zero cutoff case, by increasing the distance h, $E_W \to 0$.
- in the limit $h \to 0$, E_W^0 diverges. However, E_W remains finite in this limit.
- in the limit $h \to \infty$, E_W becomes zero which has the same behavior as in the zero cutoff case.
- $E_W \geq \frac{I(A,B)}{2}$ is valid for all values of the cutoff.

EWCS for $d_e \neq 1$

$$E_W = \frac{R^d L^{d-1}}{4 G_N r_F^{\theta} (d_e - 1)} \left[\frac{1}{r_t(h)^{d_e - 1}} - \frac{1}{r_t(2\ell + h)^{d_e - 1}} \right].$$

EWCS for $d_e \neq 1$

$$E_W = \frac{R^d L^{d-1}}{4 G_N r_F^{\theta} (d_e - 1)} \left[\frac{1}{r_t(h)^{d_e - 1}} - \frac{1}{r_t(2\ell + h)^{d_e - 1}} \right].$$

For the zero-cutoff case, one has

$$E_W^0 = \frac{R^d L^{d-1}}{4 G_N r_F^{\theta} (d_e - 1)} (2\Upsilon)^{d_e - 1} \mathcal{E}(d_e - 1),$$

where

$$\mathcal{E}(n) = \frac{1}{h^n} - \frac{1}{(2\ell + h)^n}.$$

EWCS for $d_e \neq 1$

$$E_W = \frac{R^d L^{d-1}}{4 G_N r_F^{\theta} (d_e - 1)} \left[\frac{1}{r_t(h)^{d_e - 1}} - \frac{1}{r_t(2\ell + h)^{d_e - 1}} \right].$$

For the zero-cutoff case, one has

$$E_W^0 = \frac{R^d L^{d-1}}{4 G_N r_F^{\theta} (d_e - 1)} (2\Upsilon)^{d_e - 1} \mathcal{E}(d_e - 1),$$

where

$$\mathcal{E}(n) = \frac{1}{h^n} - \frac{1}{(2\ell + h)^n}.$$

similar to the $d_e = 1$ case, E_W^0 is infinite when $h \to 0$. Furthermore, in the limit $h \to \infty$, it becomes zero. Moreover, it is independent of the cutoff.

EWCS for $d_e \neq 1$

$$E_W = \frac{R^d L^{d-1}}{4 G_N r_F^{\theta} (d_e - 1)} \left[\frac{1}{r_t(h)^{d_e - 1}} - \frac{1}{r_t(2\ell + h)^{d_e - 1}} \right].$$

For the zero-cutoff case, one has

$$E_W^0 = \frac{R^d L^{d-1}}{4 G_N r_F^{\theta} (d_e - 1)} (2\Upsilon)^{d_e - 1} \mathcal{E}(d_e - 1),$$

where

$$\mathcal{E}(n) = \frac{1}{h^n} - \frac{1}{(2\ell + h)^n}.$$

similar to the $d_e = 1$ case, E_W^0 is infinite when $h \to 0$. Furthermore, in the limit $h \to \infty$, it becomes zero. Moreover, it is independent of the cutoff.

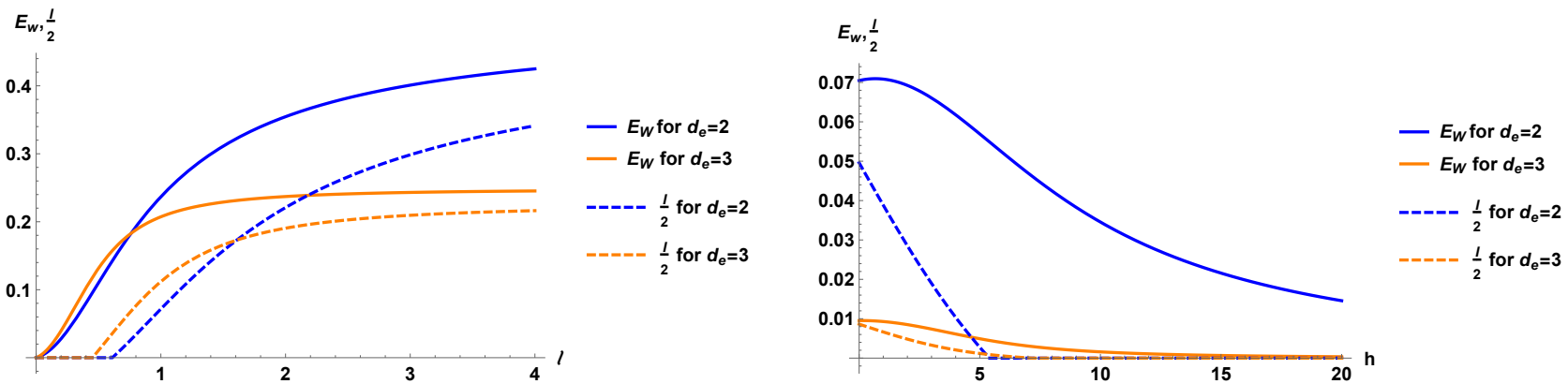

Figure: *Left)* $h = 0.1$ and $r_c = 1$. *Right)* $\ell = 10$ and $r_c = 5$.

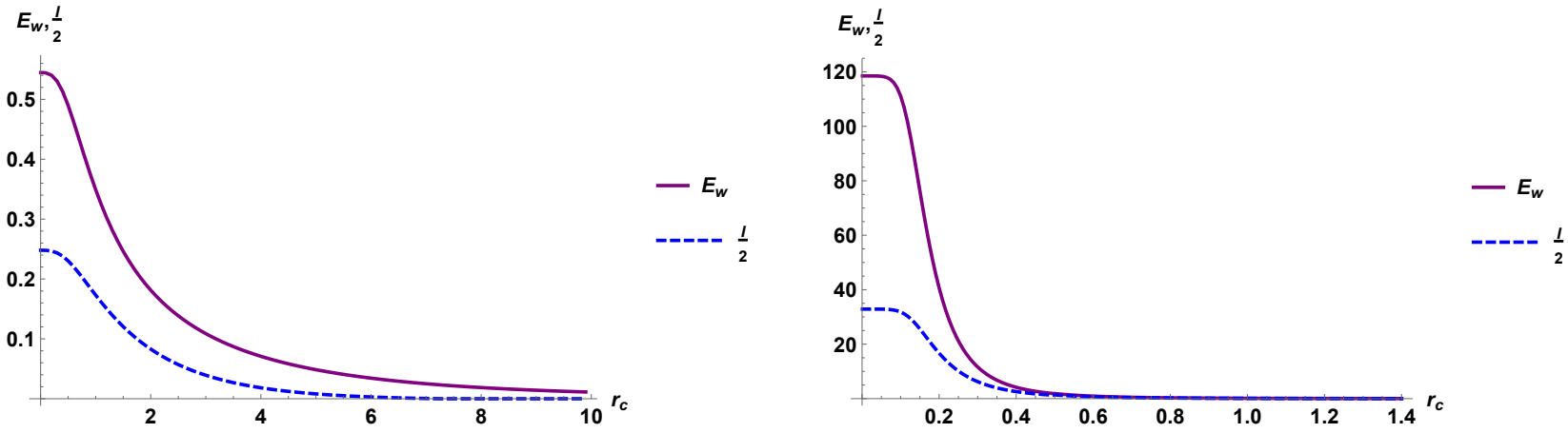

Figure: *Left*) $\ell = 5,\ h = 1$ and $d_e = 2$. *Right*) $\ell = 1,\ h = 0.1$ and $d_e = 5$.

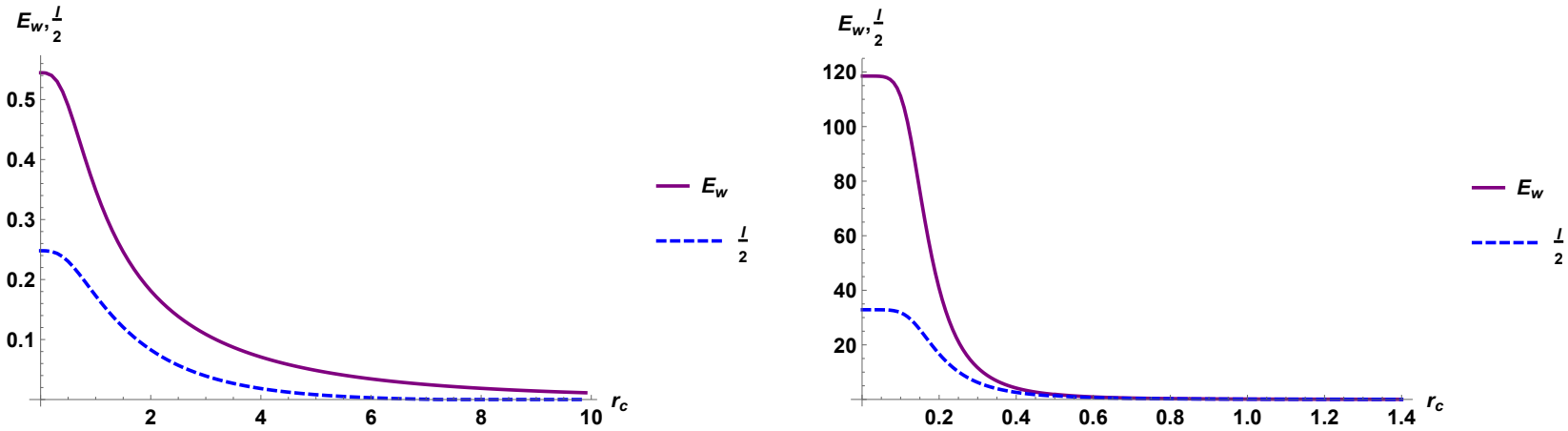

Figure: *Left*) $\ell = 5$, $h = 1$ and $d_e = 2$. *Right*) $\ell = 1$, $h = 0.1$ and $d_e = 5$.

- It is a decreasing function of the cutoff.

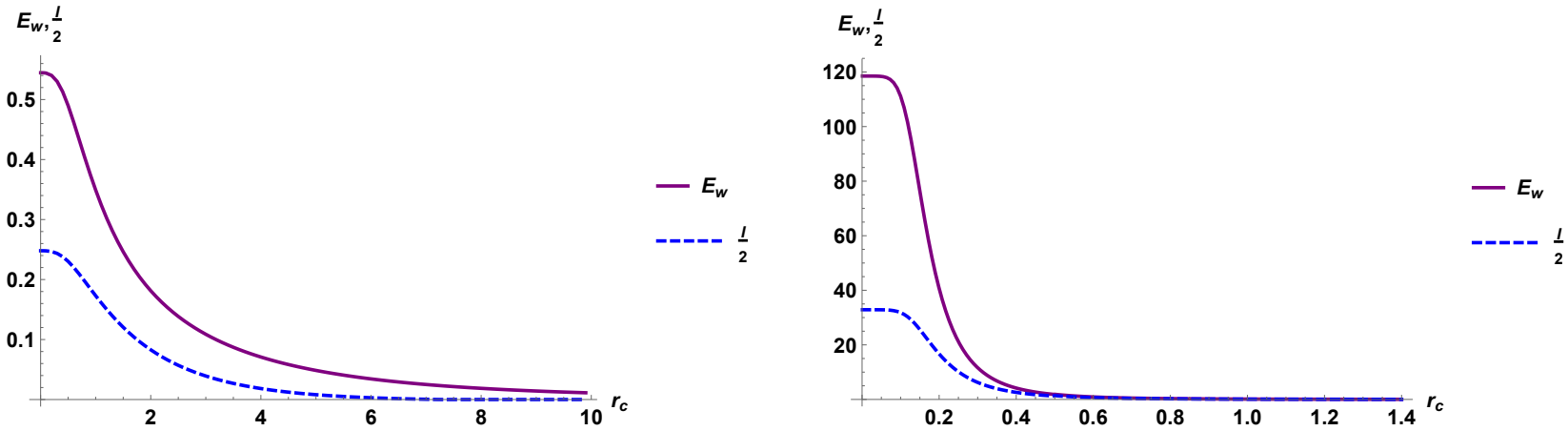

Figure: *Left*) $\ell = 5$, $h = 1$ and $d_e = 2$. *Right*) $\ell = 1$, $h = 0.1$ and $d_e = 5$.

- It is a decreasing function of the cutoff.
- It is finite when $r_c \to 0$, and goes to zero when $r_c \to \infty$.

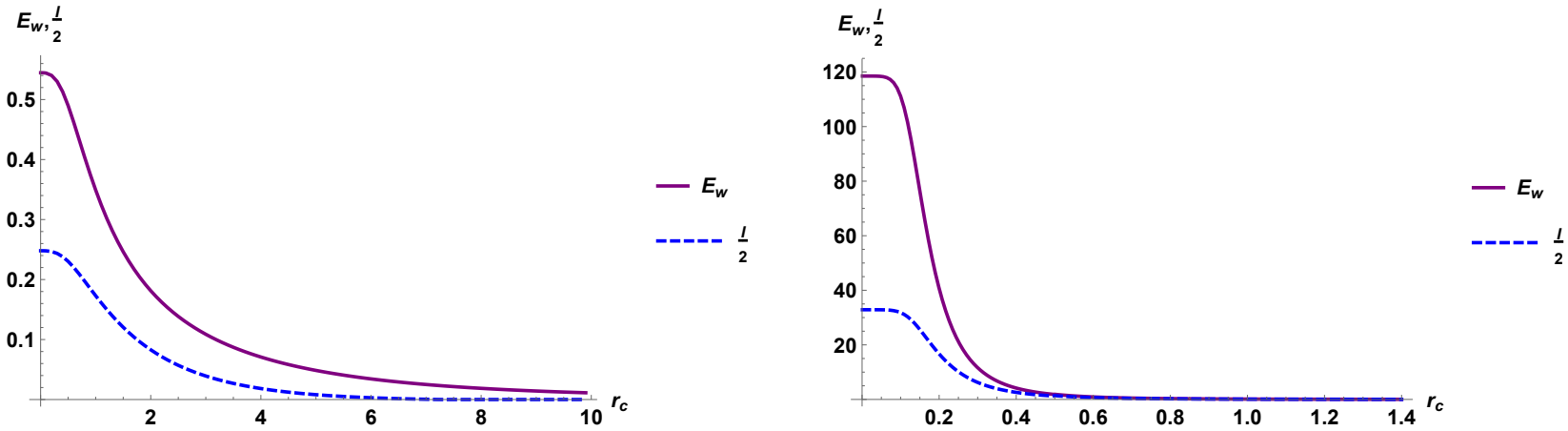

Figure: *Left*) $\ell = 5$, $h = 1$ and $d_e = 2$. *Right*) $\ell = 1$, $h = 0.1$ and $d_e = 5$.

- It is a decreasing function of the cutoff.
- It is finite when $r_c \to 0$, and goes to zero when $r_c \to \infty$.
- $E_W \geq \frac{I(A,B)}{2}$ is valid for all values of the cutoff.

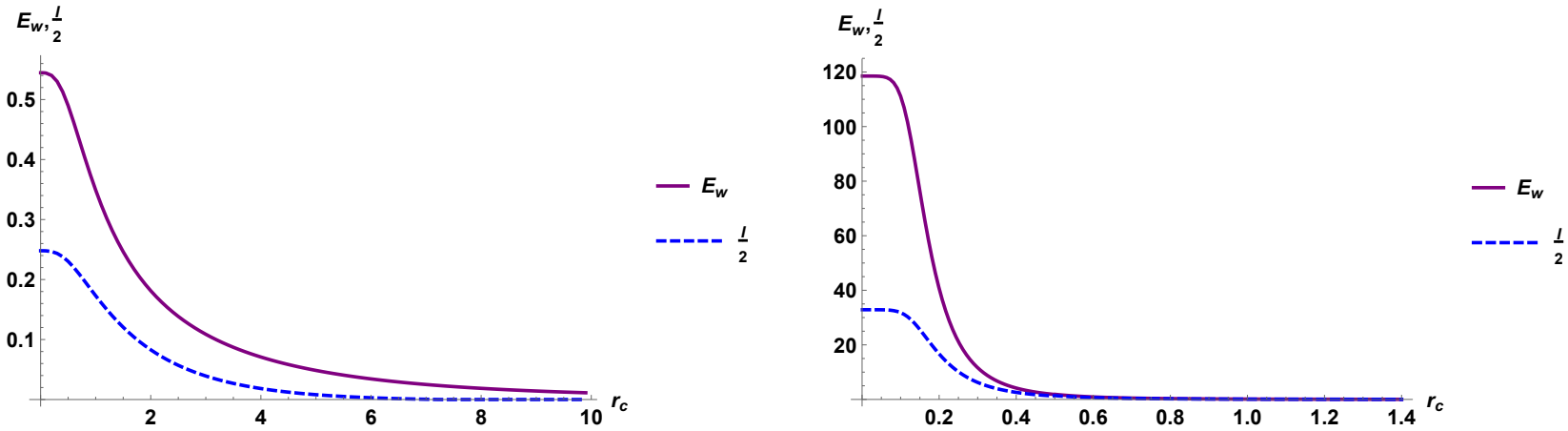

Figure: *Left*) $\ell = 5$, $h = 1$ and $d_e = 2$. *Right*) $\ell = 1$, $h = 0.1$ and $d_e = 5$.

- It is a decreasing function of the cutoff.
- It is finite when $r_c \to 0$, and goes to zero when $r_c \to \infty$.
- $E_W \geq \frac{I(A,B)}{2}$ is valid for all values of the cutoff.

On the other hand, one can find analytic expressions for very large and small entangling regions.

Very small cutoff $(\ell, h \gg r_c)$**:** one can find $\Delta E_W = E_W - E_W^0$ as follows

$$\Delta E_W = \frac{R^d L^{d-1} (2\Upsilon)^{d_e-1}}{4 G_N r_F^\theta (d_e+1)} \Bigg[-\Upsilon^{d_e} (2r_c)^{d_e+1} \mathcal{E}(2d_e) + \frac{d_e}{(d_e+1)} \Upsilon^{2d_e} (2r_c)^{2(d_e+1)} \mathcal{E}(3d_e+1)$$
$$- \frac{d_e(3d_e+1)}{3(d_e+1)^2} \Upsilon^{3d_e} (2r_c)^{3(d_e+1)} \mathcal{E}(2(2d_e+1))$$
$$+ \frac{d_e(2d_e+1)(3d_e+1)}{6(d_e+1)^3} \Upsilon^{4d_e} (2r_c)^{4(d_e+1)} \mathcal{E}(5d_e+3) + \cdots \Bigg].$$

when $r_c = \epsilon \to 0$, it becomes zero.

Very small cutoff $(\ell, h \gg r_c)$**:** one can find $\Delta E_W = E_W - E_W^0$ as follows

$$\Delta E_W = \frac{R^d L^{d-1} (2\Upsilon)^{d_e-1}}{4 G_N r_F^\theta (d_e+1)} \Big[-\Upsilon^{d_e} (2r_c)^{d_e+1} \mathcal{E}(2d_e) + \frac{d_e}{(d_e+1)} \Upsilon^{2d_e} (2r_c)^{2(d_e+1)} \mathcal{E}(3d_e+1) - \frac{d_e(3d_e+1)}{3(d_e+1)^2} \Upsilon^{3d_e} (2r_c)^{3(d_e+1)} \mathcal{E}(2(2d_e+1)) + \frac{d_e(2d_e+1)(3d_e+1)}{6(d_e+1)^3} \Upsilon^{4d_e} (2r_c)^{4(d_e+1)} \mathcal{E}(5d_e+3) + \cdots \Big].$$

when $r_c = \epsilon \to 0$, it becomes zero.

Very large cutoff $(\ell, h \ll r_c)$**:** one finds

$$E_W = \frac{R^d L^{d-1}}{32 G_N r_F^\theta} \frac{d_e}{r_c^{d_e-1}} \Big[-\frac{\mathcal{E}(-2)}{r_c^2} + \frac{d_e(d_e+5)}{48} \frac{\mathcal{E}(-4)}{r_c^4} - \frac{d_e^2(4d_e(d_e+1)+175)}{9216} \frac{\mathcal{E}(-6)}{r_c^6} + \frac{d_e^3(625 - 4d_e(39 + d_e(d_e-12)))}{147456} \frac{\mathcal{E}(-8)}{r_c^8} + \cdots \Big].$$

Therefore, when $r_c \to \infty$, one has $E_W \to 0$.

Conclusions:

We considered a HV geometry at finite temperature and radial cutoff which might be considered to be dual to a $T\overline{T}$-like deformed of HV QFT. We calculated HEE, HMI and EWCS for entangling regions in the shape of strips.

Conclusions:

We considered a HV geometry at finite temperature and radial cutoff which might be considered to be dual to a $T\overline{T}$-like deformed of HV QFT. We calculated HEE, HMI and EWCS for entangling regions in the shape of strips. For HEE, it was observed that:

- the turning point depends on the cutoff, in contrast to the zero cutoff case.

Conclusions:

We considered a HV geometry at finite temperature and radial cutoff which might be considered to be dual to a $T\overline{T}$-like deformed of HV QFT. We calculated HEE, HMI and EWCS for entangling regions in the shape of strips. For HEE, it was observed that:

- the turning point depends on the cutoff, in contrast to the zero cutoff case.
- HEE is a decreasing function of r_c.

Conclusions:

We considered a HV geometry at finite temperature and radial cutoff which might be considered to be dual to a $T\overline{T}$-like deformed of HV QFT. We calculated HEE, HMI and EWCS for entangling regions in the shape of strips. For HEE, it was observed that:

- the turning point depends on the cutoff, in contrast to the zero cutoff case.
- HEE is a decreasing function of r_c.

Furthermore, the HMI shows interesting behaviors:

- It is a decreasing function of the cutoff r_c, and goes to zero in the limit $r_c \to \infty$. It is in contrast to the zero cutoff case.
- It still shows a first-order phase transition, and the critical length $h_{\text{crit.}}$ becomes larger by increasing d_e. Moreover, $h_{\text{crit.}}$ depends on the cutoff and decreases by increasing r_c. It is in contrast to the zero cutoff case where $h_{\text{crit.}}$ is independent of the cutoff.
- When $h \to 0$, the HMI remains finite. It is in contrast to the zero cutoff case where the HMI diverges in the limit $h \to 0$.
- Since the HEE is independent of the dynamical exponent z, the HMI also shows the same behavior.

We also considered EWCS for two disjoint parallel strips:

- It is a decreasing function of the cutoff and goes to zero in the limit $r_c \to \infty$. It is in contrast to the zero cutoff case where E_W is independent of r_c.

We also considered EWCS for two disjoint parallel strips:

- It is a decreasing function of the cutoff and goes to zero in the limit $r_c \to \infty$. It is in contrast to the zero cutoff case where E_W is independent of r_c.
- It is a smooth function of both ℓ and h, and at the point $h_{\text{crit.}}$ where the HMI undergoes a phase transition, it does not show a discontinuous phase transition. It is in contrast to the zero cutoff case. However, at $h_{\text{crit.}}$ the concavity of E_W changes.

We also considered EWCS for two disjoint parallel strips:

- It is a decreasing function of the cutoff and goes to zero in the limit $r_c \to \infty$. It is in contrast to the zero cutoff case where E_W is independent of r_c.
- It is a smooth function of both ℓ and h, and at the point $h_{\text{crit.}}$ where the HMI undergoes a phase transition, it does not show a discontinuous phase transition. It is in contrast to the zero cutoff case. However, at $h_{\text{crit.}}$ the concavity of E_W changes.
- By increasing the distance h, E_W goes to zero, similar to the zero cutoff case. However, in the limit $h \to 0$, E_W remains finite, which is in contrast to the zero cutoff case where E_W diverges in this limit.

We also considered EWCS for two disjoint parallel strips:

- It is a decreasing function of the cutoff and goes to zero in the limit $r_c \to \infty$. It is in contrast to the zero cutoff case where E_W is independent of r_c.
- It is a smooth function of both ℓ and h, and at the point $h_{\text{crit.}}$ where the HMI undergoes a phase transition, it does not show a discontinuous phase transition. It is in contrast to the zero cutoff case. However, at $h_{\text{crit.}}$ the concavity of E_W changes.
- By increasing the distance h, E_W goes to zero, similar to the zero cutoff case. However, in the limit $h \to 0$, E_W remains finite, which is in contrast to the zero cutoff case where E_W diverges in this limit.
- $E_W \geq \frac{I(A,B)}{2}$ is satisfied for all vales of the cutoff r_c as well as ℓ and h.

We also considered EWCS for two disjoint parallel strips:

- It is a decreasing function of the cutoff and goes to zero in the limit $r_c \to \infty$. It is in contrast to the zero cutoff case where E_W is independent of r_c.
- It is a smooth function of both ℓ and h, and at the point $h_{\text{crit.}}$ where the HMI undergoes a phase transition, it does not show a discontinuous phase transition. It is in contrast to the zero cutoff case. However, at $h_{\text{crit.}}$ the concavity of E_W changes.
- By increasing the distance h, E_W goes to zero, similar to the zero cutoff case. However, in the limit $h \to 0$, E_W remains finite, which is in contrast to the zero cutoff case where E_W diverges in this limit.
- $E_W \geq \frac{I(A,B)}{2}$ is satisfied for all vales of the cutoff r_c as well as ℓ and h.
- It is independent of the dynamical exponent z.

We also considered EWCS for two disjoint parallel strips:

- It is a decreasing function of the cutoff and goes to zero in the limit $r_c \to \infty$. It is in contrast to the zero cutoff case where E_W is independent of r_c.
- It is a smooth function of both ℓ and h, and at the point $h_{\text{crit.}}$ where the HMI undergoes a phase transition, it does not show a discontinuous phase transition. It is in contrast to the zero cutoff case. However, at $h_{\text{crit.}}$ the concavity of E_W changes.
- By increasing the distance h, E_W goes to zero, similar to the zero cutoff case. However, in the limit $h \to 0$, E_W remains finite, which is in contrast to the zero cutoff case where E_W diverges in this limit.
- $E_W \geq \frac{I(A,B)}{2}$ is satisfied for all vales of the cutoff r_c as well as ℓ and h.
- It is independent of the dynamical exponent z.

Furthermore, for $z = 1$ and $\theta = 0$, the Lorentz and scaling symmetries are restored and the background becomes an AdS_{d+2} spacetime in Poincaré coordinates. Therefore, all of our results can be applied for an AdS_{d+2}, if one sets $\theta = 0$.

Thank you very much